Long-COVID cognitive impairments and reproductive hormone deficits in men may stem from GnRH neuronal death

Florent Sauve,[a,t] Sreekala Nampoothiri,[a,t] Sophie A. Clarke,[b,t] Daniela Fernandois,[a,t] Caio Fernando Ferreira Coêlho,[a,t] Julie Dewisme,[a,c] Edouard G. Mills,[b] Gaetan Ternier,[a] Ludovica Cotellessa,[a] Cristina Iglesias-Garcia,[d] Helge Mueller-Fielitz,[e] Thibaud Lebouvier,[a,f] Romain Perbet,[a,c] Vincent Florent,[a] Marc Baroncini,[a] Ariane Sharif,[a] June Ereño-Orbea,[g,s] Maria Mercado-Gómez,[g,s] Asis Palazon,[g,s] Virginie Mattot,[a] Florence Pasquier,[a,f] Sophie Catteau-Jonard,[a,h] Maria Martinez-Chantar,[g,s] Erik Hrabovszky,[i] Mercé Jourdain,[j] Dominique Deplanque,[a,k,l] Annamaria Morelli,[m] Giulia Guarnieri,[m] Laurent Storme,[n] Cyril Robil,[o] François Trottein,[o] Ruben Nogueiras,[d] Markus Schwaninger,[e] Pascal Pigny,[p,u] Julien Poissy,[l,q,u] Konstantina Chachlaki,[a,u] Claude-Alain Maurage,[a,c,l,u] Paolo Giacobini,[a,u] Waljit Dhillo,[b,r,u] S. Rasika,[a,**,u] and Vincent Prevot[a,*,u]

[a]Univ. Lille, Inserm, CHU Lille, Lille Neuroscience & Cognition, UMR-S 1172, DistAlz, Lille, France
[b]Section of Endocrinology and Investigative Medicine, Imperial College London, London, United Kingdom
[c]CHU Lille, Department of Pathology, Centre Biologie Pathologie, France
[d]CIMUS, Universidade de Santiago de Compostela, Santiago de Compostela, 15782, Spain
[e]Institute for Experimental and Clinical Pharmacology and Toxicology, University of Lübeck, Lübeck, Germany
[f]CHU Lille, Department of Neurology, Memory Centre, Reference Centre for Early-Onset Alzheimer Disease and Related Disorders, Lille, France
[g]CIC bioGUNE, Basque Research and Technology Alliance (BRTACentro de Investigación Biomédica en Red de Enfermedades Hepáticas y Digestivas (CIBERehd), Instituto de Salud Carlos III, Madrid, Spain
[h]CHU Lille, Department of Gynecology and Obstetrics, Jeanne de Flandres Hospital, F-59000, Lille, France
[i]Laboratory of Reproductive Neurobiology, Institute of Experimental Medicine, Budapest, Hungary
[j]Univ. Lille, Inserm, CHU Lille, Service de Médecine Intensive Réanimation, U1190, EGID, F-59000 Lille, France
[k]University Lille, Inserm, CHU Lille, Centre d'investigation Clinique (CIC) 1403, F-59000, Lille, France
[l]LICORNE Study Group, CHU Lille, Lille, France
[m]Department of Experimental and Clinical Medicine, University of Florence, Italy
[n]CHU Lille, Department of Neonatology, Hôpital Jeanne de Flandre, FHU 1000 Days for Health, F-59000, France
[o]University Lille, CNRS, Inserm, CHU Lille, Institut Pasteur de Lille, U1019 - UMR 9017 - CIIL - Center for Infection and Immunity of Lille, F-59000 Lille, France
[p]CHU Lille, Service de Biochimie et Hormonologie, Centre de Biologie Pathologie, Lille, France
[q]Univ. Lille, Inserm U1285, CHU Lille, Pôle de Réanimation, CNRS, UMR 8576 - UGSF - Unité de Glycobiologie Structurale et Fonctionnelle, F-59000, Lille, France
[r]Department of Endocrinology, Imperial College Healthcare NHS Trust, London, United Kingdom
[s]Bizkaia Technology Park, Building 801A, 48160, Derio, Bizkaia, Spain

eBioMedicine
2023;96: 104784
Published Online 13 September 2023
https://doi.org/10.1016/j.ebiom.2023.104784

Summary

Background We have recently demonstrated a causal link between loss of gonadotropin-releasing hormone (GnRH), the master molecule regulating reproduction, and cognitive deficits during pathological aging, including Down syndrome and Alzheimer's disease. Olfactory and cognitive alterations, which persist in some COVID-19 patients, and long-term hypotestosteronaemia in SARS-CoV-2-infected men are also reminiscent of the consequences of deficient GnRH, suggesting that GnRH system neuroinvasion could underlie certain post-COVID symptoms and thus lead to accelerated or exacerbated cognitive decline.

Methods We explored the hormonal profile of COVID-19 patients and targets of SARS-CoV-2 infection in post-mortem patient brains and human fetal tissue.

Findings We found that persistent hypotestosteronaemia in some men could indeed be of hypothalamic origin, favouring post-COVID cognitive or neurological symptoms, and that changes in testosterone levels and body weight over time were inversely correlated. Infection of olfactory sensory neurons and multifunctional hypothalamic glia called tanycytes highlighted at least two viable neuroinvasion routes. Furthermore, GnRH neurons themselves were dying in all patient brains studied, dramatically reducing GnRH expression. Human fetal olfactory and

*Corresponding author.
**Corresponding author.
E-mail addresses: vincent.prevot@inserm.fr (V. Prevot), sowmyalakshmi.rasika@inserm.fr (S. Rasika).
[t]These authors contributed equally to this work.
[u]These authors contributed equally to this work.

vomeronasal epithelia, from which GnRH neurons arise, and fetal GnRH neurons also appeared susceptible to infection.

Interpretation Putative GnRH neuron and tanycyte dysfunction following SARS-CoV-2 neuroinvasion could be responsible for serious reproductive, metabolic, and mental health consequences in long-COVID and lead to an increased risk of neurodevelopmental and neurodegenerative pathologies over time in all age groups.

Funding European Research Council (ERC) grant agreements No 810331, No 725149, No 804236, the European Union Horizon 2020 research and innovation program No 847941, the Fondation pour la Recherche Médicale (FRM) and the Agence Nationale de la Recherche en Santé (ANRS) No ECTZ200878 Long Covid 2021 ANRS0167 SIGNAL, Agence Nationale de la recherche (ANR) grant agreements No ANR-19-CE16-0021-02, No ANR-11-LABEX-0009, No. ANR-10-LABEX-0046, No. ANR-16-IDEX-0004, Inserm Cross-Cutting Scientific Program HuDeCA, the CHU Lille Bonus H, the UK Medical Research Council (MRC) and National Institute of Health and care Research (NIHR).

Keywords: COVID-19; GnRH; Neurodevelopment; Cognition; Infertility; Hypothalamus

Research in context

Evidence before this study

Neuroendocrine neurons expressing the master reproductive hormone, gonadotropin-releasing hormone (GnRH), while mostly hypothalamic, have also been shown to migrate or project to parts of the brain involved in intellectual functions, and their correct maturation is important for brain development in general. Interestingly, cognitive deficits in both individuals with Down syndrome (DS), who display olfactory deficits, premature aging and an Alzheimer disease (AD)-like neurodegenerative pathology, as well as in animal models of DS and AD, appear to be associated with the deficient expression of GnRH. In addition, menopause/andropause, when gonadotropin levels are deregulated, is also associated with altered cognitive function. GnRH insufficiency due to age or disease might thus be a widespread mechanism underlying several types of cognitive decline over time.
A significant proportion of male COVID-19 patients also display persistent low testosterone levels, reminiscent of absent or aberrant GnRH production, and SARS-CoV-2 has been shown to invade the brain. Taken together, these findings raise the possibility that in such patients, the GnRH system may be infected or dysfunctional, leading to the accelerated aging and cognitive deficits observed in patients with "long-COVID" or post-COVID syndrome. However, in what way and for how long GnRH neurons or their function may be affected in COVID-19 patients is still unknown.

Added value of this study

By studying the hormonal profile of male COVID-19 patients at different time points after infection, we found that persistent hypotestosteronaemia in some men could indeed be of hypothalamic origin, and that changes over time in testosterone levels and body weight, another physiological function regulated by the hypothalamus, were inversely correlated. Next, by looking for the targets of SARS-CoV-2 infection in post-mortem COVID-19 patient brains, we observed the infection of olfactory sensory neurons and multifunctional hypothalamic glia called tanycytes, highlighting at least two viable routes for viral entry into the brain and access to the GnRH system. Furthermore, GnRH neurons themselves were dying in all patient brains studied, dramatically reducing GnRH expression. Finally, our study of human fetal olfactory and vomeronasal epithelia, from which GnRH neurons arise, and fetal GnRH neurons indicates that GnRH neurons could also be susceptible to SARS-CoV-2 infection in fetuses or new-borns.

Implications of all the available evidence

SARS-CoV-2 is capable of invading the hypothalamus through at least 2 distinct invasion routes. The resulting dysfunction of GnRH neurons and tanycytes could thus be responsible for serious reproductive, metabolic, and mental health consequences in long-COVID patients, and may lead to a delayed increase in the risk of neurodevelopmental and neurodegenerative pathologies in all age groups.

Introduction

The cognitive decline associated with age-related dementias, estimated to affect some 55 million people worldwide, is a growing problem in aging societies. In a ground-breaking study, we have recently shown that cognitive deficits in both individuals with Down syndrome (DS), a disorder also characterized by olfactory deficits, premature aging and an Alzheimer disease (AD)-like neurodegenerative pathology,[1] as well as in a trisomic animal model of DS,[2] are caused by the progressive loss of expression of gonadotropin-releasing hormone (GnRH) by neuroendocrine neurons in the

brain. Interestingly, although GnRH has long been considered to be merely the master hormone regulating the reproductive axis, GnRH neurons have been found to also migrate and project to brain regions implicated in intellectual functions.[2,3] Together with a similar association between GnRH and cognition in a mouse model of AD,[2] as well as the known association between menopause/andropause or gonadotropin levels and altered cognitive function,[4–8] these results suggest that GnRH insufficiency due to age or disease might be a widespread mechanism underlying several types of cognitive decline with age.[9]

COVID-19 infection also appears to be associated with accelerated aging and an increased risk of neurodegenerative conditions such as AD in affected patients.[10–14] In addition, despite the continued emergence of new variants of SARS-CoV-2, "long COVID" or "post-COVID-19 syndrome", rather than acute infections, is becoming the major preoccupation from both the healthcare and economic points of view. While definitions of "long COVID" vary, a significant proportion of individuals infected with SARS-CoV-2 continue to experience symptoms consistent with reports of neuroinvasion by the virus, including fatigue, cognitive difficulties or "brain fog", headaches and persistent anosmia, from several months to more than a year after the initial infection.[15–18] Interestingly, a significant proportion of male COVID-19 patients also display low testosterone levels that can persist for months after recovery from infection, reminiscent of absent or aberrant GnRH production or secretion and the dysfunction of the hypothalamic-pituitary-gonadal (HPG) axis.[19,20]

In light of the potentially serious population-wide repercussions of post-COVID-19 GnRH loss for age-related cognitive decline and accelerated or exacerbated neurodegeneration in the decades to come, we explored the link between these different signs and brain infection by SARS-CoV-2 using human COVID-19 patient blood samples, post mortem brains, fetal tissues and cell lines.

Methods

Ethics authorizations

All human tissues were obtained in accordance with French laws (Good Practice Concerning the Conservation, Transformation, and Transportation of Human Tissue to Be Used Therapeutically, published on December 29, 1998). Informed consent was obtained from all patients involved in the study.

Adult COVID-19 patient brains and blood samples and control brains were obtained under authorization for the GonadoCOVID study (French protocol # 2-20-056 id8504) and authorized by the Lille Neurobiobank.

The Imperial College London study was performed in accordance with the Declaration of Helsinki with ethical approval granted by the London Bridge Research Ethics Committee (REC ref 20/HRA/4110) and was registered on the ISRCTN Trial Registry (ISRCTN15615697. All participants provided written informed consent prior to inclusion in the study.

The studies on human fetal tissue were approved by the French agency for biomedical research (Agence de la Biomédecine, Saint-Denis la Plaine, France, protocol no: PFS16-002). Non-pathological human fetuses were obtained at GW7, GW11 and GW14 from voluntarily terminated pregnancies after written informed consent from the donors (Gynaecology Department, Jeanne de Flandre Hospital, Lille, France).

COVID-19 ICU patient blood sample and hormonal analysis (CHU Lille)

Sixty male patients, 35–82 years of age, admitted to the resuscitation unit of the Lille University Hospital with a positive COVID-19 PCR were included in the "GonadoCOVID" study (French protocol # 2-20-056 id8504). Exclusion factors were a previous history of cancer or cirrhosis. Due to the difficulty of following the menstrual cycles of female patients in the ICU, female patients were excluded. For each patient, blood samples yielding 2000 µl of serum were obtained during the first week following admission, at 2 weeks and at 4 weeks if still hospitalized. The sampling week was defined based on the day the samples were obtained, where D1, D3, D5 sampling days were grouped to Week 1; D7, D9, D14 to week 2 and D30 to week 4. Sixteen patients died while in the ICU. Patient profiles are provided in Table S1.

The patients were categorized into four groups based on the severity of the decrease in testosterone (T) and LH levels (Group 1 = testosterone <2.88 ng/ml with LH ≤ 2 IU/L, Group 2 = testosterone <2.88 ng/ml with LH > 2 but <12 IU/L, Group 3 = testosterone <2.88 ng/ml with LH > 12 IU/L, Group 4 = testosterone >2.88 ng/ml).

Control ICU patient blood sample and hormonal analysis (CHU Lille)

Non-COVID-19 infected ICU patients (n = 50) used as controls belonged to the READIAB study (PHRC 2007 of the French Ministry of Health and Social Affairs: READIAB-G4; ClinicalTrials.gov: NCT03055169), a prospective, observational, multicentre study conducted from April 2012 to August 2016 in the ICUs of six French hospitals. Enrolled patients were aged 28–87 years and admitted to the ICU for at least two organ failures, defined according to sequential organ failure assessment (SOFA) scores. Pregnant women, patients admitted for <48 h, and patients who, or whose family members/surrogates, did not give their consent were excluded. Blood samples were obtained during a 3-day observational period while the patients were in the ICU.

Post-COVID-19 patient blood sample and hormonal analysis (Imperial College London)

Male participants for this study were recruited from a cohort of patients who attended Imperial College

Healthcare NHS Trust with a clinical suspicion of COVID-19 between March and November 2020. Additional participants were recruited via advertisements placed on social media asking for patients who had tested positive for COVID-19. All participants attended at least 3 months following diagnosis with COVID-19. Participants were aged ≥18 years with a diagnosis of COVID-19 confirmed using either real-time RT-PCR testing of a nasopharyngeal swab, confirmatory imaging (chest radiograph or computed tomography scan), or a positive serum SARS-CoV-2 IgG antibody test taken after symptom onset. Exclusion criteria included those prescribed steroids following recovery from COVID-19. Patient profiles are provided in Table S2.

Participants (n = 47) attended for their study visit at least 3 months following their initial presentation with COVID-19. This was part of a wider study[21] evaluating adrenal and thyroid function in COVID-19 survivors. Participants were non-fasting and study visits commenced between 8:00 and 9:30 AM to control for circadian hormonal changes. Participants (n = 22) attended for a second follow-up visit more than 1 year after presentation with COVID-19 for a repeat measurement of serum LH, FSH and testosterone.

Serum LH, FSH and testosterone were measured using automated chemiluminescent immunoassays (Abbott Diagnostics, UK). Intra-assay and inter-assay coefficients of variation were as follows: LH, <5%; FSH, <5%; total testosterone, <5%; cortisol, <10%. Limits of detection for each assay were as follows: LH in international units per litre (IU/L), 0.07; FSH in IU/L, 0.05; total testosterone in nanomoles per litre (nmol/L).

COVID-19 patient and control brains

The brains of 4 subjects (3 males and 1 female) who died of COVID-19 infection in the Lille University Hospital and 5 control subjects (4 males and 1 female) who did not test positive for COVID-19, including 2 who died before the pandemic began, were used for this study. COVID-19 and control subjects were matched for age, sex and comorbidities as far as possible. Their clinical characteristics are summarized in Table 1.

In keeping with strict protocols regarding the treatment of SARS-CoV-2-infected human tissues, human brains were immersion-fixed in 10% formalin for 1 week at room temperature. The hypothalamus was then dissected out and immersion-fixed in 4% paraformaldehyde in PBS 0.1 M, pH 7.4, for an additional 48 h at 4 °C, cryoprotected in 30% sucrose for an additional week at 4 °C, embedded in Tissue-Tek and frozen in liquid nitrogen at the crystallization temperature of isopentane.

Human fetuses

Non-pathological human fetuses (7, 11 and 14 gestational weeks (GW), n = 1 per developmental stage) were obtained from voluntarily terminated pregnancies after written informed consent was obtained from the parents (Gynaecology Department, Jeanne de Flandre Hospital, Lille, France). Fetuses were fixed by immersion in 4% PFA at 4 °C for 5 days. The tissues were then cryoprotected in PBS containing 30% sucrose at 4 °C overnight, embedded in Tissue-Tek OCT compound (Sakura Finetek), frozen on dry ice, and stored at –80 °C until sectioning. Frozen samples were cut serially at 20 µm intervals with a Leica CM 3050 S cryostat (Leica Biosystems Nussloch GmbH) and immunolabelled as described below.

COVID-19 patient and control nasal epithelia

The olfactory epithelia of 3 deceased patients (2 COVID-19 patients and 1 control) were collected at the Lille University Hospital. Their clinical characteristics are summarized in Table 1.

Tissues were formalin-fixed in 10% formalin for at least 1 week at room temperature, then decalcified by immersion in ethylenediaminetetraacetic acid (EDTA) 20%, pH 7.4, 3 times for 48 h. After that, they were immersed in 30% sucrose at 4 °C until they sank, for cryoprotection. Finally, they were embedded in Tissue-Tek, frozen in liquid nitrogen and cut into 20 µm-thick sections.

FNC-B4 fetal human GnRH neuronal cell line

FNC-B4 cells[22] were kept in culture in Coon's modified Ham's F12 medium complemented with 10% FBS at 37 °C and 5% CO2 and medium was changed twice weekly. Cells were used for pseudoviral infection and gene expression analysis when they reached 70% confluency. Gene expression assays for GnRH, ACE2, and NRP1 were carried out on uninfected cells by quantitative RT-PCR.

Pseudotyped viral particle infection of cultured FNC-B4 cells for flow cytometry and immunocytofluorescence

Pseudotyped viral particles used for the infection were constructed according to the method detailed in Crawford et al., 2020[23] using a five-plasmid system lentiviral backbone 10 (CMV promoter to express ZsGreen Fluorescent Protein), the SARS-CoV-2 spike protein, HDM-Hgpm2, pRC-CMV-Rev1b and HDM-tat1b. Cells infected with the viral particles emit green fluorescence due to the expression of ZsGreen, allowing their detection by flow cytometry. FNC-B4 cells were infected by treatment with 1.1 × 104 viral particles per mL in conditioned medium for 36 h. Cells were then trypsinized, pelleted at 1000 g for 5 min and resuspended in PBS for flow cytometry. Flow cytometry was performed using a CytoFLEX LX flow cytometer (Beckman Coulter). The gating strategy was based on measurements of green fluorescence by comparing cell

suspensions from green-fluorescence positive cells and negative cells. For each replicate, green positive events were counted from a total of 50,000 events.

For immunocytofluorescence, FNC-B4 cells were plated on cover glasses coated with 0.01% Poly-L-lysine at low confluency. Cells were fixed in 4% PFA for 15 min and stored at 4 °C in PBS containing 0.05% sodium azide. Prior to primary antibody incubation, non-specific binding sites were blocked and cells permeabilized using an incubation solution (0.3% Triton, 0.3% BSA in PBS, pH 7.4) for an hour at room temperature. Cells were then incubated with the primary antibodies (Antibody table) in incubation solution overnight at 4 °C. After three washes with PBS, cells were incubated with secondary antibodies (Antibody table) in incubation solution for an hour at room temperature. After three washes, cells were counterstained with DAPI and mounted in Mowiol.

SARS-CoV-2 infection of FNC-B4 cells

Viral infection experiments were carried out in a biosafety level 3 (BSL3) facility at the Institut Pasteur de Lille campus and complied with current national and institutional regulations and ethical guidelines (Institut Pasteur de Lille/B59-350,009). The cells were seeded in 24-well plates with pre-coated coverslips (40,000 cells/w). 3 days later the cells were counted before infection and then infected at MOI 1, 2, and 5 with SARS-CoV-2 variant D614G for 1 h. After 1 h the inoculum was removed, the cells were rinsed with PBS, and then recultured for 24 h in fresh medium. In some wells, to increase infection efficiency, trypsin-TPCK (1 µg/mL) was added to the fresh medium. After 24 h, the supernatant was kept for TCID50 viral load testing and the cells were rinsed with PBS 1X and fixed with 4% paraformaldehyde for 30 min followed by several rinses with PBS before labelling. All experiments were performed within the biosafety level 3 suite.

RNA extraction and quantitative RT-PCR analyses

For cultured human FNC-B4 cells, total RNA extraction was performed with the E.Z.N.A. Total RNA Kit I (cat: R6834-02, Omega Bio-tek, Inc.) according to the manufacturer's instructions. For human brain samples, total RNA was extracted from two fixed unstained hypothalamic slides (18 µm each) using the ReliaPrep FFPE Total RNA Miniprep System (cat: Z1002, Promega). RNA samples were immediately quantified using a Nanodrop apparatus and stored at –80 °C until the reverse transcription step. For gene expression analyses, total RNA samples were reverse transcribed using the High-capacity cDNA Reverse Transcription kit (Applied Biosystems ref 4,368,814). For fixed human brain samples, a linear preamplification step was performed using the TaqMan PreAmp Master Mix Kit protocol (Applied Biosystems ref 4,488,593). Real-time PCR was then carried out using TaqMan Universal Master Mix II

Patient	Group	Age	Sex	BMI	Time between first positive PCR and death (days)	Time between the first positive PCR and first negative one (days)	ICU stay duration (days)	Post mortem delay (hours)	Cause of death	Associated cause of death	Comorbidities
1[a]	Ctrl	69	M	31	NA	NA	27	21	Septic shock due to Fournier's gangrene	Supra and sub tentorial ischemic injuries	Peripheral arterial disease, chronic glaucoma
2[a]	Ctrl	62	M	?	NA	NA	25	19	Septic shock due to Candida fungemia	Fournier's gangrene due to rectal adenocarcinoma, Mesencephalic injuries	Stroke, arterial hypertension, dyslpidemia
3[a]	Ctrl	64	F	?	NA	NA	NA	27	Unknown, probably due to a hemorrhagic shock following a psoas hemorrhage	Subacute cholecystis; extensive peritoneal, retroperitoneal and perirenal psoas hematoma	Arterial hypertension, atrial fibrillation, aortic infectious endocarditis
4[a]	Ctrl	36	M	?	NA	NA	NA	80	Massive left ventricular infarction, extended to the interventricular septum	Atherosclerosis	Atherosclerosis
5[a]	Ctrl	50	M	?	NA	NA	NA	16	?	?	Epilepsy, dyslipidemia, ischemic heart disease
6[a,b]	COVID	63	M	30	39	29	40	45	Multi-organ failure	Lung parenchyma damage (>75%) requiring ECMO, multiple septic shock	Basedow's Disease
7[a,b]	COVID	82	M	28	67	NA	0	96	Disturbance of vigilance	Meningeal hemorrhage	Sensory neuropathy of all limbs, atrial fibrillation with left atrial closure, arterial hypertension, cerebral amyloid angeitis ?
8[a]	COVID	63	F	20	55	Positive at death	25	17	Septic shock in context of refractory hypoxia	Invasive pulmonary aspergillosis, lung parenchyma damage (25–50%)	Granulomatosis with polyangiitis
9[a]	COVID	59	M	30	74	73	46	24	Septic shock	Multiple hemorrhagic and ischemic brain injuries, diffuse meningeal hemorrhage, multiple lacunae in the basal ganglia	Arterial hypertension
10[b]	Ctrl	74	F	26	NA	NA	NA	24	Septic context	Huntington disease	Diabetes, arterial hypertension, dyslipidemia, hematopoietic stem cell transplant

[a]Patients and controls for whom brain tissues were analysed (hypothalamus and/or olfactory bulb). [b]Patients and control for whom the olfactory epithelium was analysed.

Table 1: **Clinical characteristics of control and COVID-19 patients whose post mortem brains were used in the study.**

(Applied Biosystems ref 4,440,049) on the Applied Biosystems 7900HT Fast Real-Time PCR System. The TaqMan probes used in this study are listed in Table S3.

The 18S ribosomal RNA was used as the housekeeping transcript for normalization. SARS-CoV-2 N-protein expression was assessed using the CDC 2019-Novel Coronavirus Real-Time RT-PCR Diagnostic Panel, as described elsewhere.[24,25] All gene expression data were analysed using the 2-ΔΔCt method.

RNAscope labelling

Expression of the SARS-Cov2 S-protein in post mortem brains was assessed using an RNAscope® Multiplex Fluorescent Reagent kit v2 Assay and the V-nCov2019-S probe, reference: 848,561 (both from Advanced Cell Diagnostics Inc.). Briefly, 20 µm-thick hypothalamic sections were cut on a cryostat, slides washed twice for 10 min in Gibco® DPBS (ThermoFisher) and dry baked in a HybEZ™ II oven (Advanced Cell Diagnostics Inc.) at 60 °C for 30 min. They were then immersion-fixed in 4% paraformaldehyde PBS 0.1 M, pH 7.4, prepared in DEPC-treated water, for 1 h at 4 °C and washed again twice for 10 min in Gibco® DPBS. Next, the sections were processed according to manufacturer's instructions (ethanol dehydration, RNAscope hydrogen peroxide treatment and target retrieval), incubated with RNAscope protease IV for 10 min at room temperature, and the signal revealed using the RNAscope multiplex fluorescent assay.

Immunohistochemistry and quantification for viral and host-cell markers in human tissues

Dissected, postfixed and cryoprotected blocks of adult human patient brains containing the hypothalamus or olfactory bulb were cut into 20 µm sections and mounted. A citrate-buffer antigen retrieval step, 10 mM Citrate in TBS-Triton 0.1% pH 6 for 30 min at 70 °C, was performed on 20 µm sections. After 3 washes of 5 min with TBS-Triton 0.1%, sections were blocked in incubation solution (10% normal donkey serum, 1 mg/ml BSA in TBS-Triton 0.1% pH 7, 4) for 1 h. Blocking was followed by primary antibody incubation (Table 2) in incubation solution for 48 h at 4 °C. Primary antibodies were then rinsed out, before incubation in fluorophore-coupled secondary antibodies or, in case of amplified immunolabelling biotinylated secondary antibodies for 1 h in TBS-Triton 0.1% at room temperature. For classic immunohistochemistry, secondary antibodies were washed and sections counterstained with DAPI (D9542, Sigma). For amplified immunohistochemistry, after secondary antibodies were rinsed, sections were incubated with VECTASTAIN® Elite ABC-HRP kit (PK-6100, Vector laboratories) following manufacturer's instructions. Sections were then incubated with biotinyl-tyramide reagent (SAT700001EA, PerkinElmer) following manufacturer's recommendations, washed and incubated with fluorophore-coupled streptavidin (1/500 dilution in TBS-Triton 0.1%) before counterstaining with DAPI. Finally, the sections were incubated with Autofluorescence Eliminator Reagent (2160, Millipore) following manufacturer's instructions and mounted with Fluoromount™ (F4680, Sigma). Immunolabelling in the human brain using the two antibodies to human ACE2 (R&D Systems, with tyramide amplification, and Abcam, without amplification), labelled similar cells.

For immunolabelling of human fetuses, 20 µm-thick sections of entire heads at GW 7, GW 11 and GW 14 were processed as follows. Slides first underwent antigen retrieval for 20 min in a 5 mM citrate buffer heated to 90 °C, then were rinsed in TBS and blocked/permeabilized for 2 h at room temperature in TBS +0.3% Triton +0.25% BSA +5% Normal Donkey Serum ("Incubation solution", ICS). Sections were then incubated with primary antibodies (Table 2) for two nights at 4 °C in ICS. After rinses in TBS, the sections were incubated with secondary antibodies for 2 h at room temperature in ICS, then rinsed again in TBS. Finally, nuclei were stained with DAPI (Sigma D9542, 1:5000 in TBS) for 5 min, and sections were rinsed before coverslipping with homemade Mowiol.

For immunolabelling of mouse brain sections, 30 µm-thick floating sections were rinsed 4 times in 0.1 M PBS pH 7.4 and blocked for 1 h at room temperature in blocking solution (PBS containing 10% normal donkey serum and 0.3% Triton X-100). Sections were incubated overnight at 4 °C with a mix of primary antibodies diluted in blocking solution (Table 2). The sections were washed three times in 0.1 M PBS and incubated at room temperature for 1 h with Alexa Fluor-conjugated secondary antibodies (1:500 dilution; all purchased from Molecular Probes, Invitrogen, San Diego, CA) in blocking solution. A biotin-streptavidin amplification step was added for TMPRSS2 to verify expression in some tissues. The sections were then rinsed 3 times in 0.1 M PBS. Nuclei were counterstained by incubating the sections for 1 min in DAPI before mounting and coverslipping as above. Information on the antibodies used is listed in Table 2.

Statistics

Statistical comparisons were carried out using GraphPad Prism 8. All correlations were performed using *R stats version 4.2.1*. Testosterone, LH, and FSH were compared between the four patient groups using two-tailed unpaired t-test. For the CHU Lille cohort of COVID-19 patients, Pearson's product moment correlation of (cor.test () of R *stats* version 4.2.1) was used to estimate the strength of association between testosterone (ng/ml) vs CRP (mg/ml) in all patients irrespective of sampling week. Pearson's Chi-squared test was performed to determine the association between percentage of mortality among patients and the HPG axis status. The correlation plots and the dot plots were generated using ggplot2 version 3.4.1 in R (v 4.2.1).

Antibody	Manufacturer	Reference	RRID	Dilution	sample	Validation (references or Figures)
Goat ant-i human ACE2	R&D Systems	AF933	AB_355722	1/100	Human brain tissue	[26]
Rabbit anti- human ACE2	Abcam	Ab15348	AB_301861	1/100-1/200	Human brain tissue	[27,28]
Rabbit anti-TMPRSS2	Abcam	Ab92323	AB_10585592	1/100-1/1000	Human brain tissue	[29]
Chicken anti-vimentin	Millipore	AB5733	AB_11212377	1/500	Human brain tissue	[30]
Goat anti-TAG1	R&D Systems	AF4439	AB_2044647	1/500	Human brain tissue	[31]
Goat anti-OMP	Wako	544-10001	AB_664696	1/200	Human brain tissue	[32]
Guinea Pig anti GnRH	Erik Hrabovszky	In-house		1/3000-1/6000	Human brain tissue & Cells	[33]
Mouse anti-dsRNA	SCICONS J2	1001050	AB_2651015	1/500	Human brain tissue	Fig. 3c and d
Mouse anti-SARS-CoV-2 spike protein	GeneTex	GTX632604	AB_2864418	1/200	Human brain tissue	Figure S2
Rabbit anti-SARS nucleocapsid protein	Novus Bio	NB100-56576	AB_838838	1/100	Human brain tissue	Fig. 3c and d
Goat anti-NRP1	R&D Systems	AF566	AB_355445	1/100	Human brain tissue & Cells	[34,35]
Rabbit anti-cleaved caspase 3	Cell Signalling	#9664	AB_2070042	1/200	Human brain tissue	[36]

Table 2: **List of the primary antibodies used for imunofluorescence.**

For the Imperial College London cohort, the relationship between admission CRP and testosterone was determined using Spearman's rank correlation. Testosterone levels measured in the acute phase were compared by WHO severity group using the Kruskal–Wallis test.

For quantitative RT-PCR experiments (n = 5 control patients vs 4 SARS-CoV-2-infected patients; n = 3 mock infected mice vs 5 SARS-CoV-infected mice), a two-tailed unpaired t-test was used to compare expression levels between infected and control brains. The Friedman multiple comparison test followed by an uncorrected Dunn's post hoc test was used to compare gene expression levels between the cortex, OB and hypothalamus of infected mice.

For the quantification of the proportion of GnRH neurons showing normal or abnormal morphology in control and COVID-19 patients, a two-way ANOVA was used, followed by Sidak's post hoc test (n = 18 and 20 sections, 85 and 116 GnRH neurons, respectively; n = 4 patients per group). To compare the proportion of GnRH neurons with normal or abnormal morphology that expressed cleaved caspase 3 in COVID-19 patients, a two-sided Fisher's exact test was used (n = 66 GnRH neurons, n = 4 patients).

Data from flow cytometry experiments were compared using an unpaired t-test.

Role of funders

The funding sources for this project played no role in the study design, data collection, analysis, interpretation, writing, or editing of the manuscript.

Results

When the HPG axis functions correctly, GnRH released by neurons into pituitary portal blood vessels underlying the median eminence of the hypothalamus is carried to the anterior pituitary, where it elicits the secretion of the gonadotropins, luteinizing hormone (LH) and follicle-stimulating hormone (FSH), which then act on the gonads to stimulate steroid hormone production and gametogenesis.[37] Feedback from gonadal steroids then influences the further release of GnRH and gonadotropins, such that low gonadal steroid levels would trigger a compensatory increase in LH and FSH levels, and vice versa.[38] In order to verify whether the HPG axis was functioning correctly in COVID-19 patients, we thus retrospectively measured plasma testosterone, and LH and FSH concentrations, which serve as surrogates for GnRH release, in a cohort of 60 male COVID-19 patients, 35–82 years old, hospitalized in the intensive care unit (ICU) of the Lille Medical University Hospital (CHU Lille) (Table S1**)**. During their first week in the ICU, 57 patients (Groups 1–3) showed testosterone levels that were moderately low (0.92–2.88 ng/ml) or severely low, indicative of hypogonadism (<0.92 ng/ml), while only 3 patients showed normal or near-normal testosterone levels (>2.88 ng/ml; Group 4) (Fig. 1a). Of the 57 patients with low testosterone levels, only 6 (Group 3) showed the compensatory increase in LH expected when the HPG axis functions normally (>12 IU/L) (Fig. 1b), while 38 patients (Group 2) showed intermediate concentrations of LH (2–12 IU/L) and 13 patients (Group 1) showed very low LH concentrations (<2 IU/L), indicating an impairment of the HPG axis (Fig. 1b). Of these, 10 of 13 patients (Group 1) and 15 of 38 patients (Group 2) had severely low testosterone levels (<0.92 ng/ml, indicating the existence of hypogonadotropic hypogonadism) (Fig. 1a and b). Patients with normal or near-normal testosterone levels (Group 4) all had the expected intermediate concentrations of LH (2–12 IU/L) (Fig. 1b). FSH levels broadly followed a similar pattern to that of LH (Fig. 1c). Surprisingly, given previous reports of a correlation between the intensity of the inflammatory response and low testosterone levels,[39] the level of C-reactive protein (CRP), an indicator of inflammation, was not found to be a

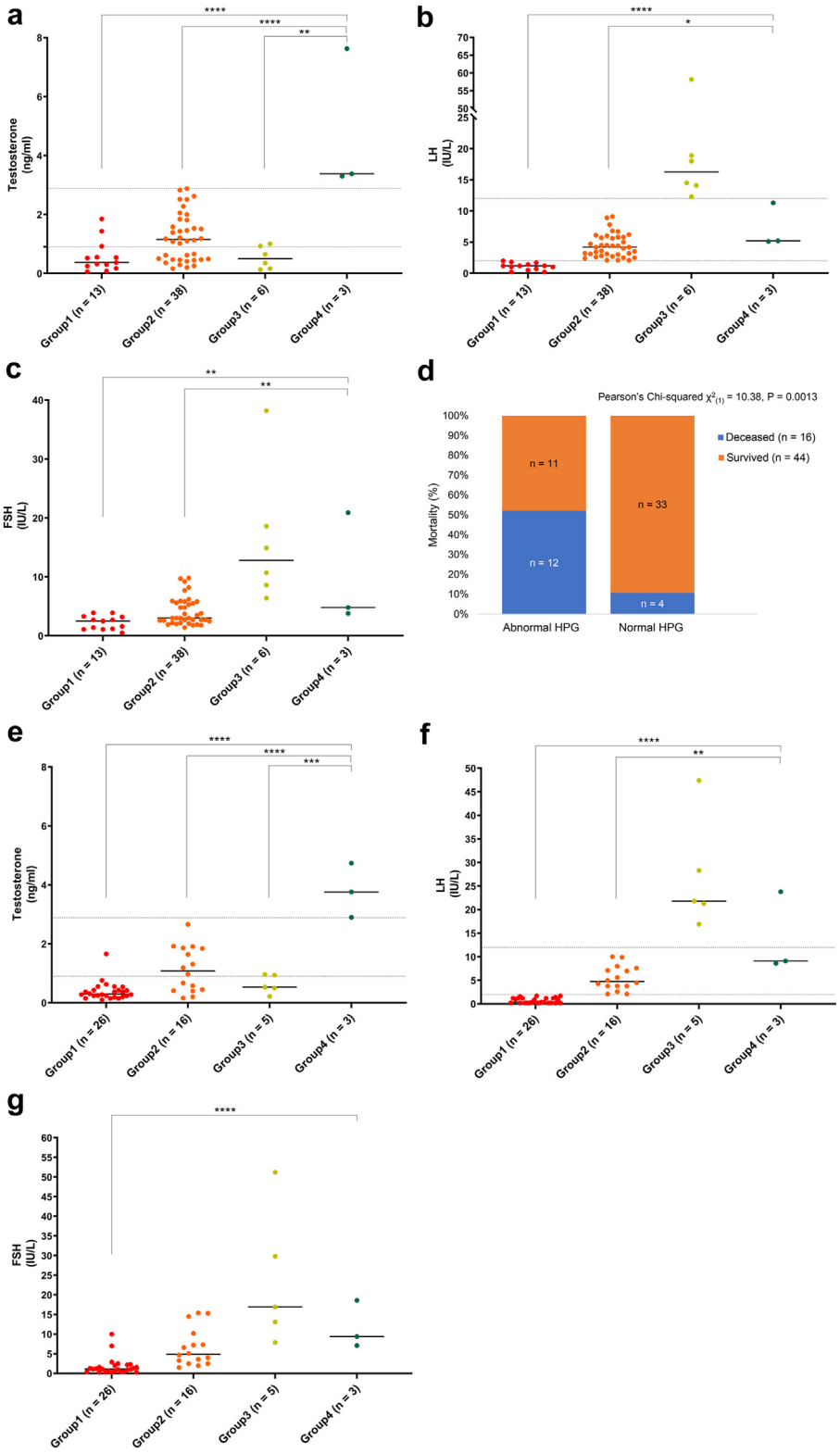

Fig. 1: **Serum testosterone, and gonadotropin (LH & FSH) concentrations in a male patients hospitalized in the intensive care unit (ICU) of the Lille Medical University Hospital (CHU Lille).** (a–d) COVID-19 infected patients in the ICU were divided into 4 groups depending on

confounding factor for hypogonadism (Figure S1a, Table S4).

COVID-19 patients who underwent an extended ICU stay were also sampled at weeks 2 and 4 in the ICU (Figure S1b and c). In these, the functioning of the HPG axis was seen to switch between "normal" (Groups 3 and 4), i.e., where testosterone levels provided feedback to LH levels, and "abnormal" (Groups 1 and 2), i.e., where LH levels were not appropriate for testosterone levels (Fig. 1a and b). Among the 16 patients who died (26.6%), HPG axis function was abnormal in 12 (75%) at the time of death (Figure S1b), whereas this condition was seen in only 11 out of 44 (25%) of the patients who survived (Figure S1c) (mortality associated with abnormal HPG function, Pearson's Chi-squared $\chi^2_{(1)} = 10.38$, $p = 0.0013$) (Fig. 1d). Together, these results suggest that the severely low total testosterone levels seen in the majority of COVID-19 patients in the ICU and the associated risk of mortality are not just a reflection of gonadal insufficiency but of impaired hypothalamic GnRH function, or hypogonadotropic hypogonadism, which may also underlie the poor prognosis reported in men with low testosterone levels.[40,41]

However, hospitalization in the ICU could itself suppress GnRH release and lead to transient hypogonadotropic hypogonadism.[42,43] To verify whether this could be the case in our patients, in the absence of uninfected control patients hospitalized in the ICU from the same period, we reanalysed testosterone, LH and FSH concentrations obtained from 50 male ICU patients from the READIAB study, aged 28–87 years, before the emergence of COVID-19. Unfortunately, 42 of these non-COVID-19 ICU patients (84%) also displayed hypogonadotropic hypogonadism according to the criteria used above (Fig. 1e–g).

In order to distinguish between HPG axis suppression as a result of the ICU stay and that due to a durable loss of GnRH following SARS-CoV-2 infection, we performed similar analyses in another cohort of 47 male patients followed at Imperial College London, 3 months or more after contracting COVID-19 (Table S2). Of these patients, 11 still had low total testosterone at this delayed time point (median days since initial presentation: 217) (Fig. 2a). None of the 11 had a compensatory increase in LH, instead having either low LH levels of <2 IU/L (4/11 patients) or normal LH levels of 2–12 IU/L (7/11 patients), indicating a persistent dysregulation of the HPG axis in 23% of men (Fig. 2b); FSH levels were mostly normal (Fig. 2c). There was no correspondence between HPG status at this delayed time point and WHO disease severity rating during the acute phase (Figure S1d). As in the Lille cohort, CRP values were not a confounding factor for HPG axis status (Figure S1e). However, the patients displayed a slight but significant increase in body weight between diagnosis and the first follow-up visit (two-tailed paired t test, $t_{(14)} = 3.025$, $p = 0.0091$).

Testosterone levels and other parameters were measured in 22 of these male patients at a second follow-up visit more than 1 year after presentation with COVID-19 (median days since initial presentation: 464; median days since first post-COVID visit: 237 days). Interestingly, all 7 patients with abnormal HPG axis function (Groups 1 or 2) during the first visit who attended the second follow-up now displayed normal testosterone levels (Group 4) (Fig. 2d). Two men displayed extremely low total testosterone levels (<2.88 ng/ml) without compensatory high LH levels (Fig. 2e), again confirming that hypogonadism in these patients might be of hypothalamic origin. These data suggest that COVID-19 infection can lead to persistent or delayed hypogonadotropic hypogonadism more than a year later in some patients. Interestingly, neither of the two men with hypotestosteronaemia at the second visit had displayed low testosterone levels at the first. A similar delayed decrease in testosterone levels was also

total testosterone and LH levels, where Group 1 = testosterone <2.88 ng/ml with LH ≤ 2 IU/L, Group 2 = testosterone <2.88 ng/ml with LH > 2 but <12 IU/L, Group 3 = testosterone <2.88 ng/ml with LH > 12 IU/L, Group 4 = testosterone >2.88 ng/ml. A two-tailed unpaired t-test was used to estimate the significance of the difference between groups (total n = 60 patients) during their first week in the ICU. (a) Testosterone (two-tailed unpaired t-test, Group 4 (n = 3) vs Group 1 (n = 13), t (14) = 6.195, ****p < 0.0001; Group 4 (n = 3) vs Group 2 (n = 38), t (39) = 6.124, ****p < 0.0001; Group 4 (n = 3) vs Group 3 (n = 6), t (7) = 4.392, **p = 0.0032 (b) Luteinizing hormone (LH) (two-tailed unpaired t-test Group 4 (n = 3) vs Group 1 (n = 13), t (14) = 6.616, ****p < 0.0001; Group 4 (n = 3) vs Group 2 (n = 38), t (39) = 2.333, *p = 0.0249; Group 4 (n = 3) vs Group 3 (n = 6), t (7) = 1.460, p = 0.1877 (c) *Follicle-stimulating* hormone (FSH) (Group 4 (n = 3) vs Group 1 (n = 13), t (14) = 3.137, **p = 0.0073; Group 4 (n = 3) vs Group 2 (n = 38), t (39) = 2.977, **p = 0.0050; Group 4 (n = 3) vs Group 3 (n = 6), t (7) = 0.8167, p = 0.4410) (d) Percentage of mortality among patients with normal (n = 37) and abnormal HPG status (n = 23). Pearson's Chi-squared test with Yates' continuity correction, X2 (1) = 10.38, p = 0.0013 (e–g) Non-COVID-19 male ICU patients (n = 50) were divided into 4 groups depending on total testosterone and LH levels, where Group 1 = testosterone <2.88 ng/ml with LH ≤ 2 IU/L, Group 2 = testosterone <2.88 ng/ml with LH > 2 but <12 IU/L, Group 3 = testosterone <2.88 ng/ml with LH > 12 IU/L, Group 4 = testosterone >2.88 ng/ml. A two-tailed unpaired t-test was used to estimate the significance of the difference between groups (total n = 50 patients). (e) Testosterone (two-tailed unpaired t-test, Group 4 (n = 3) vs Group 1 (n = 26), t (27) = 14.45, ****p < 0.0001; Group 4 (n = 3) vs Group 2 (n = 16), t (17) = 5.399, ****p < 0.0001; Group 4 (n = 3) vs Group 3 (n = 5), t (6) = 7.346, ***p = 0.0003 (f) Luteinizing hormone (LH) (two-tailed unpaired t-test, Group 4 (n = 3) vs Group 1 (n = 26), t (27) = 8.926, ****p < 0.0001; Group 4 (n = 3) vs Group 2 (n = 16), t (17) = 3.495, **p = 0.0028; Group 4 (n = 3) vs Group 3 (n = 5), t (6) = 1.654, p = 0.1493 (g) *Follicle-stimulating* hormone (FSH) Group 4 (n = 3) vs Group 1 (n = 26), t (27) = 6.139, ****p < 0.0001; Group 4 (n = 3) vs Group 2 (n = 16), t (17) = 1.635, p = 0.1204; Group 4 (n = 3) vs Group 3 (n = 5), t (6) = 1.134, p = 0.2999.

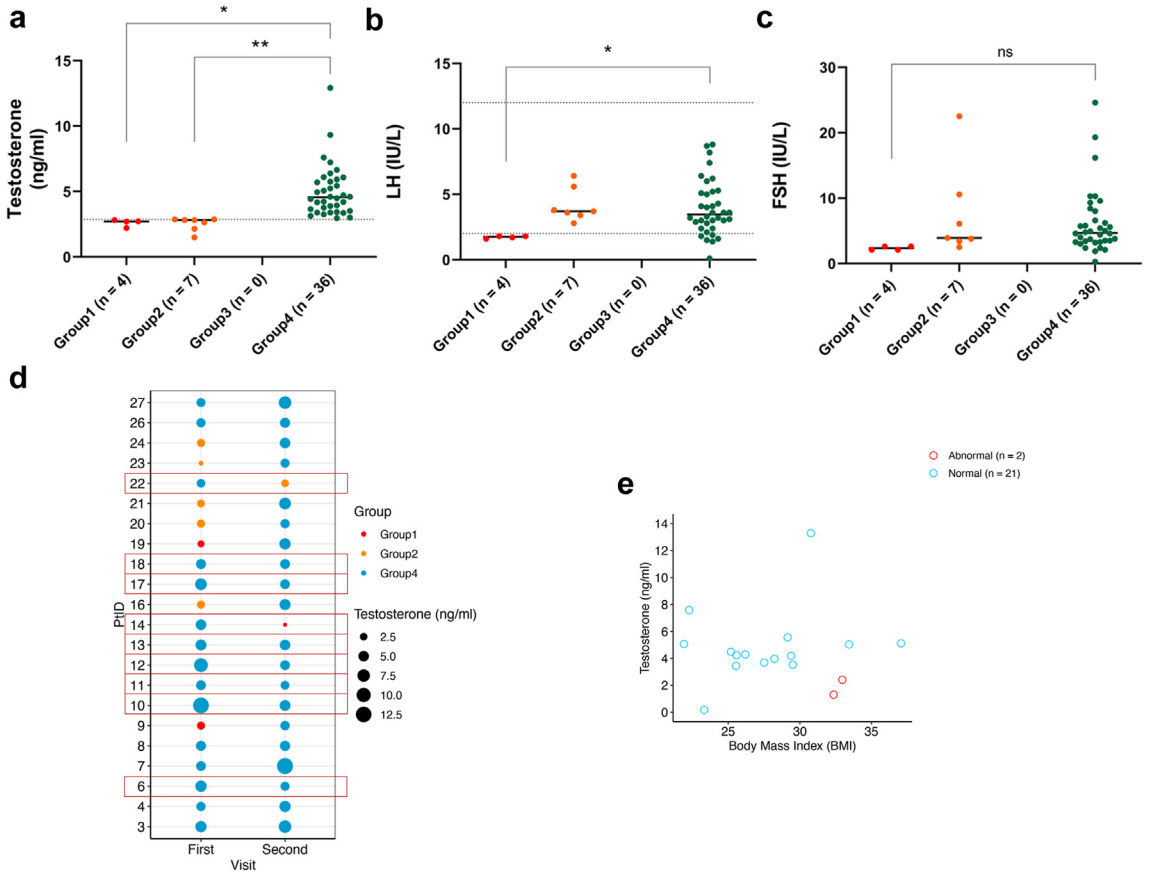

Fig. 2: **Serum testosterone, and gonadotropin (LH & FSH) concentrations in male patients followed at Imperial College London 3 months after contracting COVID-19**. COVID-19 infected male patients (n = 47) were divided into 4 groups depending on total testosterone and LH levels, where Group 1 = testosterone <2.88 ng/ml with LH ≤ 2 IU/L, Group 2 = testosterone <2.88 ng/ml with LH > 2 but <12 IU/L, Group 3 = testosterone <2.88 ng/ml with LH > 12 IU/L, Group 4 = testosterone >2.88 ng/ml. A two-tailed unpaired t-test was used to estimate the significance of the difference between groups (total n = 47 patients). (a) Testosterone (two-tailed unpaired t-test, Group 4 (n = 36) vs Group 1 (n = 4), t (38) = 2.384, *p = 0.0222; Group 4 (n = 36) vs Group 2 (n = 7), t (41) = 3.262, **p = 0.0022. (b) Luteinizing hormone (LH) (two-tailed unpaired t-test, Group 4 (n = 36) vs Group 1 (n = 4), t (38) = 2.093, *p = 0.0431; Group 4 (n = 36) vs Group 2 (n = 7), t (41) = 0.2810, p = 0.7801. (c) *Follicle-stimulating* hormone (FSH) (two-tailed unpaired t-test, Group 4 (n = 36) vs Group 1 (n = 4), t (38) = 1.535, p = 0.1330; Group 4 (n = 36) vs Group 2 (n = 7), t (41) = 0.6067, p = 0.5474. (d) Testosterone levels of patients between visits. The colour of the dot represents the HPG axis status (Group1 in red, Group 2 in orange, and Group4 in blue). The size of the dot is representative of the testosterone levels (ng/ml). Except Pt 14 and Pt 22 who switched to Group1/Group 2, all other patients were in Group 4 in the follow-up visit (median days since initial presentation: 464; median days since first post-COVID visit: 237 days). The 9 patients who displayed lower testosterone levels during the second visit than the first are outlined. (e) Testosterone levels at the second visit and the BMI of patients. Two men, both of whom had a BMI above 30, displayed extremely low total testosterone levels without compensatory high LH levels. The colour of the dot represents the HPG axis status (abnormal in red (n = 2) and normal in blue (n = 21)).

observed in 9 other patients from Group 4 (Fig. 2d), indicating a progressive dysfunction of varying severity of the HPG axis in a subpopulation of infected patients.

Hypogonadotropic hypogonadism due to SARS-CoV-2 neuroinvasion could be caused by the loss of GnRH neurons or by deficient or abnormal GnRH synthesis and release due to a perturbation of the transcription factor or cell network regulating its production.[44,45] In humans, neurons secreting GnRH constitute a sparse population of barely a couple of thousand cells,[3] principally located in the infundibular nucleus of the tuberal region of the hypothalamus.[3,46] Their neuroendocrine terminals contact fenestrated vessels of the pituitary portal system underlying the median eminence to secrete the hormone, in a process controlled by the remodelling of a specialized population of hypothalamic glia, the tanycytes. Unlike other hypothalamic neurons driving bodily functions, GnRH neurons are not born in the brain but originate in the olfactory placode, from where they migrate into the brain during embryogenesis,[47,48] while remaining in contact with the olfactory bulb (OB) via long dendrites.[3,49] GnRH neurons might

thus be exposed to SARS-CoV-2 either through the olfactory route or through the hematogenic route at the level of the median eminence in patients with viremia.

In order to determine whether GnRH neurons could be exposed to SARS-CoV-2 in COVID-19 patients, we looked for the presence of viral proteins and RNA in the brains of four patients who died of COVID-19 in the ICU in 2020, including one who displayed viremia at the time of death (Table S1), and compared them with the brains of four age-matched uninfected patients (deceased before the pandemic or with negative nasal swab PCR results), using primer pairs and antibodies specific to early SARS-CoV-2 variants and validated previously in brain tissue from the K18-hACE2 mouse model of SARS-CoV-2 infection.[50] We observed that all three of the four COVID-19 patients for whom the median eminence was available, including the one with viremia, had readily detectable levels of N-protein transcripts in the hypothalamus (Fig. 3a). Next, perfecting a technique for multiplex fluorescent in situ hybridization (RNAscope) in the hypothalamus in human brain tissue fixed in paraformaldehyde for longer than a week, we detected S-protein transcripts in vessels, some neuron-like cells and cells of the ependymal wall, while such labelling was absent in control patients despite the strong visualization of positive-control U6 mRNA (Fig. 3b).

Two host-cell factors are important for SARS-CoV-2 viral entry into a number of cell types: angiotensin-converting enzyme 2 (ACE2), which is bound by S-protein, and transmembrane protease, serine 2 (TMPRSS2), which cleaves S-protein, allowing this binding to take place. Immunofluorescence labelling for SARS-CoV-2 viral proteins and these two host-cell factors also revealed abundant N-protein and double-stranded RNA (dsRNA) in numerous cells of the median eminence/infundibular nucleus of COVID-19 patients (Fig. 3c and d), unlike uninfected controls (Fig. 3c), indicating robust SARS-CoV-2 entry and replication. However, while N-protein was often colocalized with vimentin-immunoreactive tanycytic processes, dsRNA labelling was fainter in tanycytic cell bodies lining the ventricular wall than in the nuclei of non-tanycytic cells morphologically associated with tanycytic processes (Fig. 3c and d). Interestingly, immunolabelling for S-protein, which mediates host-cell entry,[51] was extremely high in ACE2-and TMPRSS2-coexpressing tanycytic endfeet, which contact fenestrated capillaries at the external pial surface of the median eminence (Fig. 3e and f). Tanycytic endfeet are known to ensheathe and dynamically interact with GnRH axon terminals, thus controlling the periodic secretion of GnRH,[52] a process that could break down in infected patients and contribute to the observed HPG axis dysregulation. These findings suggest that in patients contracting COVID-19, SARS-CoV-2 was infecting hypothalamic cell types.

With regard to the olfactory route, while some reports do indicate the olfactory epithelium, in which some GnRH cell bodies may remain anchored in adulthood,[53] and olfactory bulb (OB) as ports of infection,[54,55] others have suggested that olfactory sensory neurons are not themselves very susceptible to infection, and that the propagation of the virus may be arrested in the OB by local immune mechanisms.[56,57] In our post mortem patient brains, immunofluorescence labelling showed abundant S-protein labelling along with ACE2 and TMPRSS2 in the olfactory nerve layer (ONL), where olfactory marker protein (OMP)-expressing axons from sensory neurons of the olfactory epithelium enter the OB (Figure S2a–c). In addition, viral dsRNA was present in numerous OB cells bordering the ONL and within the glomerular layer of COVID-19 patient brains, unlike controls (Figure S2c). Furthermore, in the decalcified nasal epithelium of one patient, immunolabelling for S-protein was clearly colocalized with OMP- and ACE2-positive olfactory sensory neurons (Figure S2a), indicating potential SARS-CoV-2 entry and replication along this second route of infection.

Given the anatomical relationship between GnRH neurons and both neuroinvasion routes, we next examined our post mortem patient brains for signs that GnRH neurons were themselves infected. Despite the extreme paucity of GnRH neurons and their scattered distribution in the hypothalamus, we identified GnRH neurons expressing both ACE2 and neuropilin 1 (NRP1), a semaphorin receptor that they use during embryonic life to migrate to their final destinations,[34,35,58,59] and which has been found to be a co-receptor or alternative receptor that facilitates SARS-CoV-2 host cell entry,[60–62] in all the brains studied (Fig. 4a and b). Furthermore, more than one-third of GnRH neurons in the brain of COVID-19 patients displayed a bloated or abnormal morphology rather than the typical fusiform morphology, suggesting that they were sick or dying (Fig. 4c and d); the number of such abnormal GnRH neurons was negligible in control brains (Fig. 4d). In keeping with the view that SARS-CoV-2 infection was causing the death of GnRH neurons, directly or indirectly through the infection of associated cell populations, some GnRH neurons were immunoreactive for cleaved caspase-3, an apoptosis marker expressed by other infected cells in the brain,[63] in all infected patient brains (Fig. 4c). A majority of these dying neurons also displayed an abnormal morphology (Fig. 4e). No cleaved caspase-3 labelling was noted in GnRH neurons in uninfected control brains. Interestingly, while GnRH neurons are an extremely small and scattered population in the human hypothalamus, we were able to observe a GnRH neuron positive for the viral S-protein in one patient brain (Fig. 4b). Further supporting the putative death or dysfunction of GnRH neurons on a massive scale, RT-PCR analysis of

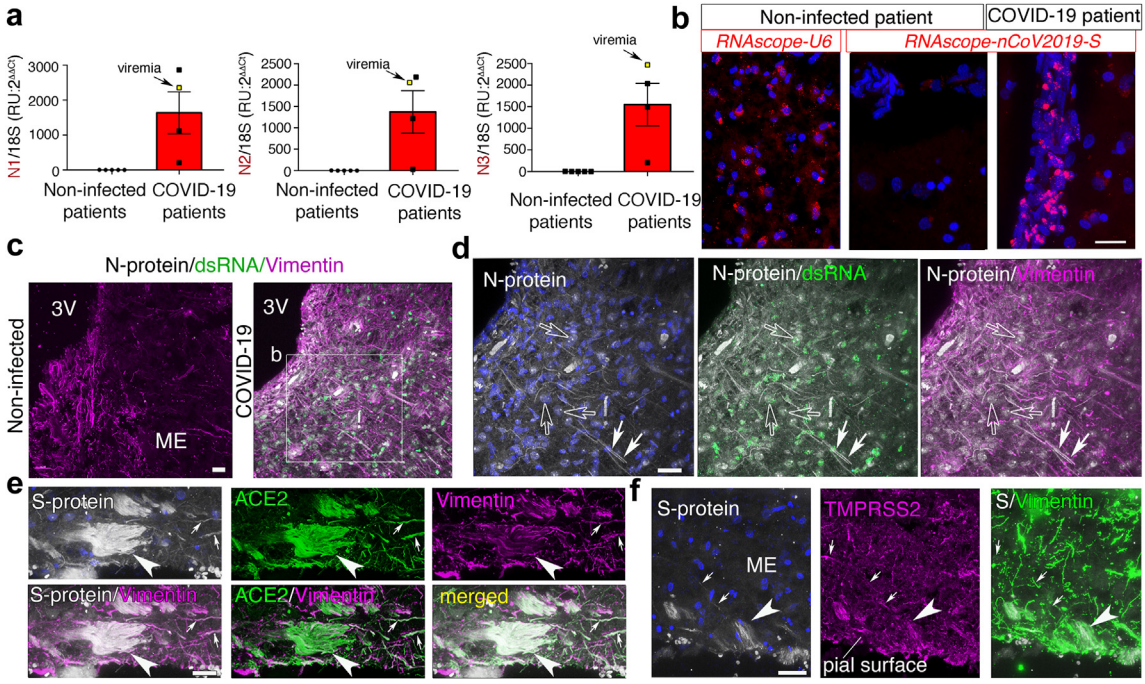

***Fig. 3:* Expression of viral transcripts and proteins, ACE2 and TMPRSS2 in the hypothalamus of COVID-19 patients and non-infected controls**. (a) Quantitative PCR analysis of N-protein mRNA in the hypothalamus of COVID-19 patients using three distinct sets of probes (N1, N2 and N3). n = 5 control patients and 4 SARS-CoV-2-infected patients. Note that one COVID-19 patient (yellow point) had viremia at the time of death. Two-tailed unpaired t test, for N1 t (7) = 3.097, p = 0.0174, for N2 t (7) = 3.143, p = 0.0163 and for N3 t (7) = 3,587, p = 0.0089). (b) RNAscope labelling for S-protein mRNA (pink) in the hypothalamus of a control (non-infected) patient and a COVID-19 patient. U6 RNA was used as a positive control. Blue: DAPI. Scale bar: 20 µm. (c) Immunolabelling for SARS-CoV-2 N-protein (white), viral dsRNA (green) and vimentin (magenta) to identify tanycytes, indicating that viral markers are absent in the hypothalamus of controls (left) but heavily expressed in a 63-year-old COVID-19 patient (right). 3 V: third ventricle. Scale bar: 30 µm. (d) N-protein (white), dsRNA (green) and vimentin (magenta) immunolabelling showing abundant N-protein colocalization with vimentin in numerous tanycytic fibres (white arrows) and its presence in non-tanycytic cell bodies (empty arrows) near the median eminence (ME). dsRNA is not present in the vimentin-rich tanycytic cell body layer lining the ventricular wall. Blue: DAPI. Scale bar: 30 µm. (e,f) Extremely strong labelling for S-protein (white) seen in the end-feet (white arrowhead) of tanycytes (vimentin; magenta in e; green in f), which also express ACE2 (green in e) and TMPRSS2 (magenta in f), at the pial surface of the ME, where tanycytic processes (white arrows) contact fenestrated capillaries. Blue: DAPI. Scale bar: 20 µm.

the hypothalamus of four COVID-19 patient brains revealed an almost complete disappearance of GnRH transcripts as compared to five control brains, whereas NRP1, which is expressed by other cell populations in the hypothalamus, was not significantly affected (Fig. 4f).

Given the importance of physiological GnRH secretion appears to have for cognitive function in adulthood,[2] to verify whether the GnRH neuronal infection and HPG axis abnormalities observed in COVID-19 patients could be associated with cognitive deficits, we analysed cognitive symptoms reported by male patients in the London cohort, who underwent extensive testing at >3 months and >1 year after infection (Table S5). At both follow-up visits, the proportion of patients reporting impaired memory or attention ("DePaul Symptom" questionnaire), regardless of frequency or severity, or difficulty concentrating ("Long COVID" questionnaire) tended to be slightly higher in the group with abnormal HPG axis function, although the patient numbers were not sufficient to draw statistically valid conclusions (100%, for n = 7 of 7 for the first visit and n = 2 of 2 for the second visit), than in the group with normal function (81%, n = 13 of 16 for the first visit; 80%, n = 16 of 20 for the second visit). A similar pattern emerged for neurological symptoms (abnormal HPG axis function: 100%, n = 7 of 7 for the first visit and n = 2 of 2 for the second visit; normal HPG axis function: 87%, n = 14 of 16 for the first visit and 90%, n = 18 of 20 for the second visit). Although these are subjective measures reported in a small sample of patients, they suggest that the time course and pathogenic mechanisms underlying the effects of neuroinvasion, and more specifically, the interplay

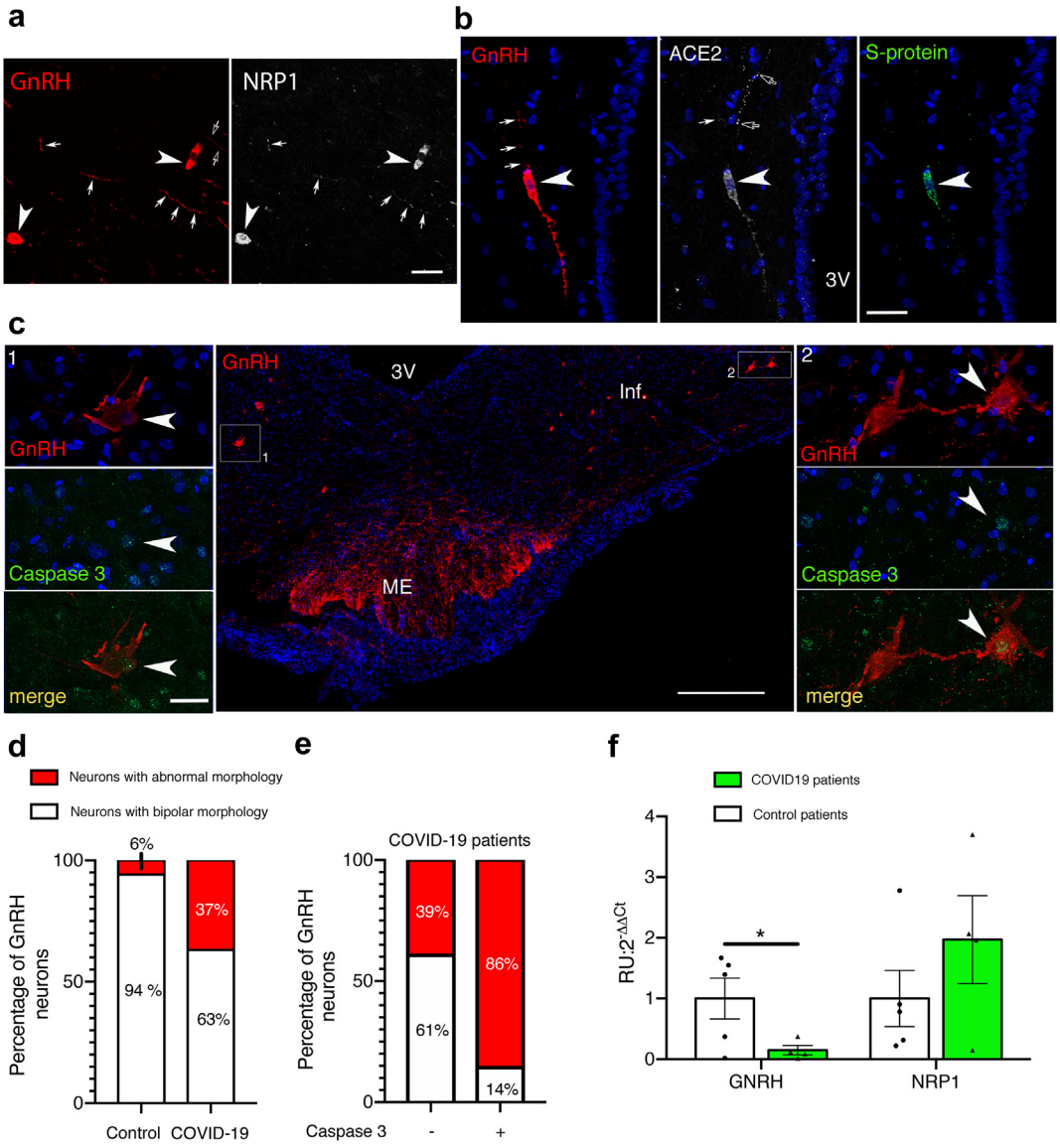

***Fig. 4:* SARS-CoV-2 infects GnRH neurons and leads to their death in COVID-19 patients**. (a) Immunolabelling for GnRH (red) and NRP1 (white) in hypothalamic GnRH neurons in a control patient. Arrowheads show a double-labelled GnRH neuron, while white arrows show a GnRH-immunoreactive process expressing NRP1. Scale bar: 50 µm. (b) Immunolabelling for GnRH (red), ACE2 (white), and S-protein (green) in hypothalamic GnRH neurons in a COVID-19 patient. Arrowheads show a triple-labelled GnRH neuron, white arrows show a GnRH-immunoreactive process that does not express ACE2, and empty arrows show an ACE2-immunoreactive neuron-like process that does not express GnRH. Blue: DAPI. Scale bar: 50 µm. (c) Immunolabelling for GnRH (red) and cleaved caspase 3 (green) in the infundibular nucleus (Inf)–median eminence (ME) area of the hypothalamus of a COVID-19 patient. Blue: DAPI. Scale bars: 500 µm (inset 30 µm). (d) Quantification of proportion of GnRH neurons showing normal or abnormal morphology in control and COVID-19 patients (two-sided Fisher's exact test, $p < 0.0001$, n = 66 GnRH neurons, n = 4 patients). (e) Proportion of cleaved caspase 3-expressing or healthy GnRH neurons with normal or abnormal morphology in COVID-19 patients (two-sided Fisher's exact test, $p = 0.0387$, n = 66 GnRH neurons, n = 4 patients). (f) Quantitative RT-PCR for GnRH and NRP1 in the infundibular nucleus-median eminence of COVID-19 and control patients showing the almost complete disappearance of GnRH expression in patients (two-tailed unpaired t-test $t(7) = 2.197$, $p = 0.0320$ for control vs COVID-19 brains. n = 5 for control patient and n = 4 for COVID-19 brains).

between HPG axis dysfunction and cognition deficits, require further large-scale retrospective or prospective investigations.

The existence of an olfactory route combined with the vulnerability of GnRH neurons to SARS-CoV-2 also raises another spectre: that of an infection of these

neurons, which are born in the nose, during embryonic development or early childhood. Indeed, the migration, maturation and correct adult function of GnRH neurons may be important not only for the establishment or maintenance of cognitive or metabolic function,[2,35,64] but could also play a role in normal or pathological aging.[2] We therefore analysed the olfactory epithelium of 7-, 11- and 14-week-old human fetuses, and found abundant expression of ACE2 and TMPRSS2 in both olfactory sensory neurons and their TAG-1-immunoreactive axons extending into the OB (Figure S3a–c), adding to previous reports of these susceptibility factors in other cell populations of the olfactory epithelium.[65] Serendipitously, neurons composing the putative vomeronasal organ,[3] the birthplace of GnRH neurons (Fig. 5a–d, Figure S3d–f), as well as the axonal tracts along which they migrate into the brain (Fig. 5e), also abundantly expressed ACE2 and TMPRSS2 as well as NRP1 (Fig. 5e), as we have previously shown,[34] potentially further favouring SARS-CoV-2 cell entry and infection of this crucial neuronal population.[60,61]

Finally, to directly verify that human fetal GnRH neurons can be infected by SARS-CoV-2, we tested the ability of pseudotyped viral particles expressing the full-length SARS-CoV-2 S-protein and the ZsGreen reporter gene[23] or the SARS-CoV-2 virus to infect a human fetal GnRH-expressing cell line, FNC-B4.[66] Interestingly, cells differentiating into GnRH neurons not only expressed susceptibility factors for infection (Fig. 5f and g), but a fraction of these cells were confirmed to be infected by the pseudovirus, using flow cytometry ($p = 0.0235$, two-tailed unpaired t-test) (Fig. 5h and i), or by SARS-CoV-2 itself, using immunocytochemistry (Fig. 5j). These experiments raise the strong possibility that at least some GnRH neurons in human fetuses or new-borns could indeed be infected by SARS-CoV-2 in case of vertical transmission from infected mothers (see for example[67,68]), with potential long-term mental and nonmental consequences later in life.

Discussion

The triad of anosmia, hypogonadism and cognitive deficits, which occurs in a significant proportion of "long COVID" cases, is also reminiscent of another disease: Down syndrome or Trisomy 21. Our recent identification of a peripubertal decline in GnRH production as the likely causative factor underlying not only the dysfunction of the gonadotropic axis but also the progressive cognitive decline and AD-like neurodegeneration observed in Down syndrome patients[2] prompted us to study whether GnRH system dysfunction due to neuroinvasion by SARS-CoV-2 could underlie some of these symptoms in COVID-19 patients. Our work demonstrates that GnRH neurons as well as other associated hypothalamic cells could indeed be infected by SARS-CoV-2 through at least two routes, and that this results in a dramatic decrease in GnRH expression in the brain. Moreover, even human fetal GnRH neurons express susceptibility factors for SARS-CoV-2 host-cell entry and can be infected by the virus. Together, this vulnerability of developing and mature GnRH neurons to SARS-CoV-2 neuroinfection creates a potential for devastating long-term effects on cognitive and metabolic aging, in addition to the expected dysfunction of the reproductive axis.

That SARS-CoV-2 invades and has profound effects on the brain is no longer in doubt, although not all parts of the brain may be equally vulnerable to infection.[69–74] Unlike some previous studies, we found ample evidence of olfactory sensory neuronal infection in the nasal epithelium of COVID-19 patients, supporting the existence of a viable route for the virus into the brain along the olfactory and terminal nerves.[75] Blood-borne SARS-CoV-2 viral particles might also directly enter the brain by extravasating from fenestrated vessels of circumventricular organs and thus bypassing the blood–brain barrier. This hypothesis is supported by the abundance of viral markers in the median eminence of the hypothalamus in the three patient brains for whom this tissue was available. Interestingly, the absence of the traditional blood–brain barrier in the median eminence, an adaptation essential to allow peptide neurohormones such as GnRH to easily reach their target cells in the pituitary and for circulating peripheral signals necessary for the establishment of homeostasis to enter the brain, could instead represent a breach in the brain's defences against pathogens. In addition, we have previously shown that endothelial cells of the blood–brain barrier are themselves infected by SARS-CoV-2, potentially allowing viral passage into the brain.[63] Indeed, recent accounts of SARS-CoV-2 brain infection put the incidence of viremia at up to 40%,[72] greatly increasing the likelihood of a viable hematogenic route for the virus. GnRH neurons, which both maintain contact with the nasal epithelium where they are born, and extend neuroendocrine terminals to the perivascular space around the fenestrated vessels of the median eminence, and which express NRP1 as well as ACE2, could thus potentially be infected by either route, or through viral propagation by adjacent cells.

The infection of either GnRH neurons themselves or of tanycytes, which interact with their terminals, would likely be sufficient to cause hypogonadotropic hypogonadism either through decreased GnRH expression, as we observed in post mortem patient brains, or perturbed secretion, as reflected by gonadotropin levels in our cohorts, although hospitalization in the ICU may itself cause a transient impairment of the HPG axis through a variety of intrinsic and extrinsic factors. However, many GnRH neurons, which normally constitute a stable population, were also bloated and dying in our COVID-19 patient brains. The irreversible loss of GnRH that would entail could thus develop along

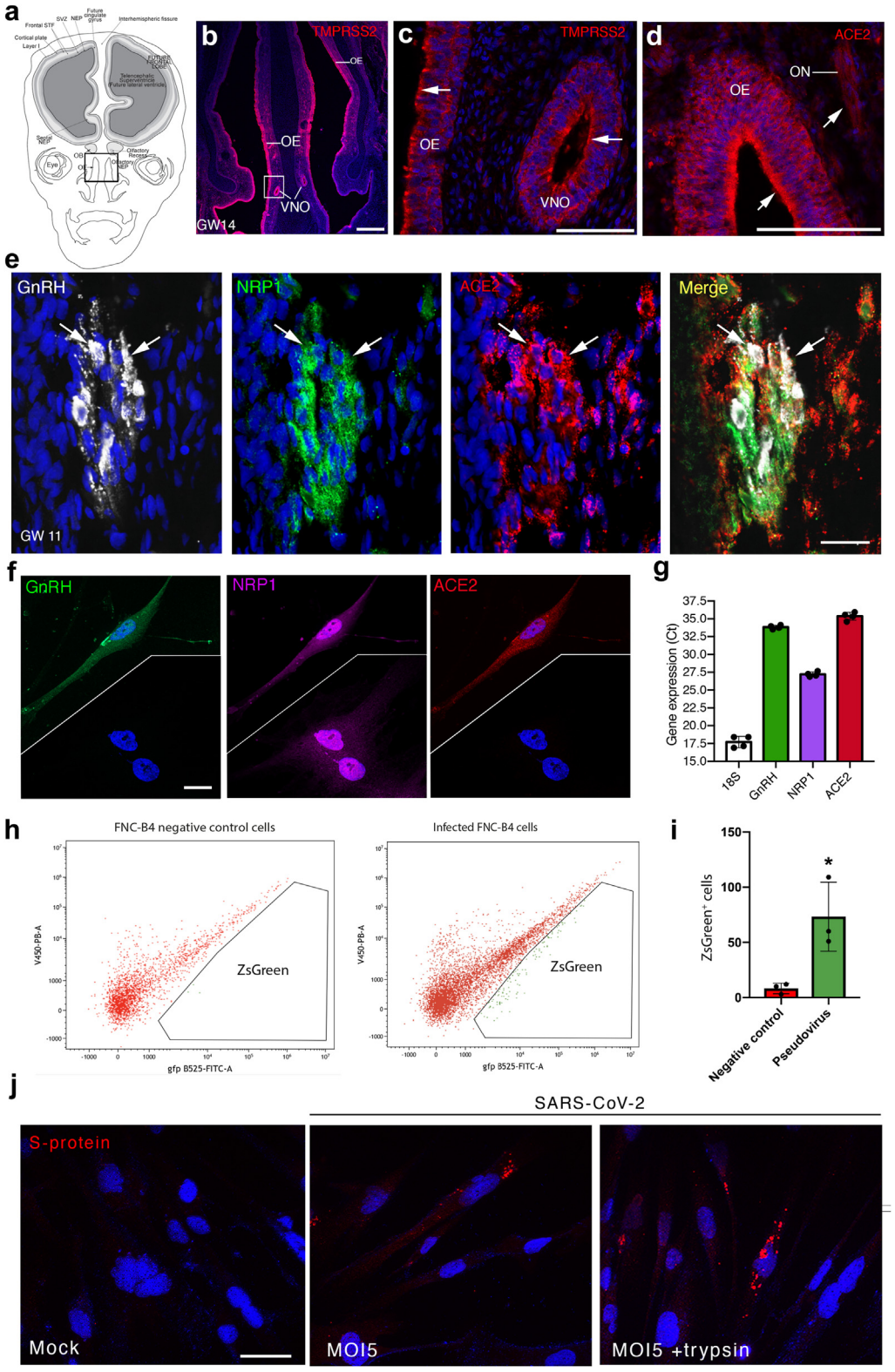

***Fig. 5:* Human fetal GnRH neurons are susceptible to SARS-CoV-2 viral infection**. (a) Schematic representation of a horizontal section through the nose and brain of a gestational week (GW) 14 human fetus, showing region immunolabelled in (b–d). (b–d) TMPRSS2 (b,c, red) and

a longer time course, a phenomenon that could be exacerbated by the recently reported persistence of active virus in the brain, including in the hypothalamus, for weeks or months after infection.[72] In light of the multiple brain functions in which GnRH seems to be involved, this impairment could have several putative deleterious effects.

The most obvious repercussion of a long-term decline in GnRH production, given the role of GnRH as the master molecule controlling the reproductive axis, is a delayed effect on fertility in both male and female patients who survive infection. This can be seen in two men from our London cohort, in whom hypogonadism developed several months after infection, and a few case reports[76,77] (see also a meta-analysis[78]). Extrapolated over the millions of infections reported worldwide, this is especially concerning considering the current global decline in human fertility, including in Europe (https://www.euro.who.int/__data/assets/pdf_file/0010/73954/EN63.pdf). Interestingly, mutations in NRP1, a molecule that can potentiate SARS-CoV-2 host cell infection,[60,61] cause Kallmann syndrome in humans, in which hypogonadotropic hypogonadism is associated with anosmia,[59] by perturbing GnRH neuronal migration.[34] A significant proportion of COVID-19 patients display anosmia or dysosmia[79] and defects in GnRH neuronal function may also be associated with alterations in olfactory perception.[2,35,44,80] It would thus be interesting to investigate whether some persistent olfactory deficits in COVID-19 patients could also be linked to the loss of GnRH.

More importantly, GnRH neurons also project to parts of the brain involved in cognition, such as the cortex or hippocampus,[2] and GnRH is involved in maintaining brain connectivity and cognitive function in adulthood, a process that breaks down with the loss of its expression.[2,81] Conversely, restoring physiological levels and patterns of GnRH improves connectivity and cognitive performance, for instance in Down syndrome patients and in an animal model of AD, while restoring a microRNA involved in GnRH expression, miR200b, also normalizes the expression of myelination genes, as well as inter-hippocampal neuronal communication,[2] providing an anatomical substrate for these changes. Interestingly, the most debilitating short- and long-term consequences of SARS-CoV-2 infection include cognitive symptoms, such as "brain fog", and demyelination, altered gene expression mimicking accelerated aging and AD-like neurodegenerative changes are among the mechanisms proposed to explain these symptoms (see for example,[10–12,71,73]). It is thus worth considering whether the dramatic downregulation of GnRH and the death of GnRH neurons in the brain of COVID-19 patients could contribute to an acceleration or exacerbation of age-related cognitive decline. In the adult brain, the loss of a substantial proportion of GnRH neurons can occur without leading to functional impairments of the reproductive axis.[82] However, the threshold for GnRH loss at which cognitive changes are triggered is not known, and it is conceivable that not only reduced GnRH expression levels but merely a dysregulation of its pulsatile pattern may lead to cognitive deficits, as seen in Down syndrome.[2] While the small patient numbers and heterogeneity of our study cohorts did not allow for in-depth measurements or valid statistical comparisons, the fact that all men in the impaired HPG axis group displayed persistent cognitive symptoms, regardless of disease severity, supports a role for GnRH loss or dysregulation in the aetiology of these symptoms. There is thus an urgent need for further studies to confirm this correlation, long-term monitoring of hormone levels as an indicator of the risk of cognitive decline in COVID-19 survivors, and an evaluation of the usefulness of GnRH replacement therapy to compensate for the deficits.

GnRH neurons are also implicated in the regulation of normal energy metabolism,[35] as are hypothalamic tanycytes to a very large extent, by transcytosing peripheral metabolic signals such as leptin and glucose from the blood to hypothalamic neurons that control food intake.[83] Survivors of COVID-19 also appear to be at higher risk of developing diabetes,[15,84] suggesting a breakdown of this tanycytic shuttle in the brain of COVID-19 patients. Several factors could contribute to this breakdown: the potential saturation of the endocytotic mechanism suggested by the extremely high signal

ACE2 (d, red) immunolabelling in the olfactory epithelium (OE), vomeronasal organ (VNO) and olfactory nerve (ON) of a GW 14 fetus. Blue: DAPI. Scale bars: 1 mm in b and 100 µm in c-d. (e) In a GW 11 human fetus, many GnRH neurons (white) migrating out of the VNO also express NRP1 (green) and/or ACE2 (red), host cell proteins that mediate SARS-CoV-2 infection (white arrows), while NRP1 and ACE2 are also expressed by some olfactory and vomeronasal nerve axons that form the scaffold for GnRH neurons. Blue: DAPI. Scale bar: 40 µm (f) Differentiating FNC-B4 cells in culture showing the presence of NRP1 (magenta) and ACE2 protein expression (red) in cells that have begun to express GnRH (green, top view). Non-GnRH cells (bottom view) also express NRP1, in keeping with the more widespread expression of this guidance molecule in the fetal nose and brain. Blue: DAPI. Scale bar: 10 µm. (g) RT-PCR analysis demonstrating the expression of mRNAs for GnRH, NRP1, and ACE2 by FNC-B4 cells. The housekeeping 18 S RNA was used as a control. n = 3 wells. (h) Fluorescence-activated cell sorting (FACS) of FNC-B4 cells (red) infected with pseudotyped lentiviral particles carrying a full-length SARS-CoV-2 spike protein and a ZsGreen reporter gene (green), showing infection of some cells by the pseudovirus. (i) ZsGreen expression, indicating pseudotyped viral particle entry, is almost undetectable in uninfected negative control cells treated only with vehicle (two-tailed unpaired t-test t (4) = 3.566 p = 0.0235, n = 3 wells). (j) Immunolabelling of the SARS-CoV-2 S-protein in FNC-B4 cells. Scale bar: 20 µm.

for SARS-CoV-2 S-protein at the endfeet of tanycytes, perturbed feedback or signalling from morbid GnRH neurons to the tanycytic endfeet with which they interact, or the inflammation of infected tanycytes by the activation of the NFκB subunit NEMO in tanycytes by circulating proinflammatory cytokines, many of which persist in "long COVID" patients.[85,86] Indeed NEMO activation is involved in inflammation-mediated anorexia in certain non-infectious diseases,[87] and the SARS-CoV-2 major protease, Mpro, cleaves NEMO,[63] setting up a tug-of-war between the competing effects of acute or persistent systemic inflammation on tanycytes and potential post-COVID-19 swings of energy metabolism. The occurrence of such perturbations is suggested by the strong inverse correlation between change in testosterone levels and change in weight between the first and second follow-up visits in our London cohort, and the emergence of two subpopulations: patients in whom both HPG axis function (i.e., GnRH secretion) and energy metabolism eventually became normal, suggesting the recovery of tanycytes, and patients with persistent hypothalamic dysfunction (Figure S4).

Finally, in light of the unusual vulnerability of fetal GnRH neurons, particular attention must also be paid to the consequences of maternal or perinatal COVID-19 infection in neonates.[88] Indeed, the growing evidence that some neonates born to infected mothers may be COVID-19-positive[89] is especially concerning since the first postnatal activation of the HPG axis, i.e., minipuberty, a phenomenon that plays a key role in the later maturation of the reproductive system[45,90] and likely also in brain development in a broader sense,[49] occurs shortly after birth. The impairment of minipuberty,[91,92] for example by premature birth,[93,94] may be correlated with the incidence of a range of age-related non-communicable diseases or metabolic dysfunction,[49,93,94] and early reports already indicate that antenatal or neonatal exposure to SARS-CoV-2 may lead to neurodevelopmental delays.[95] Studies following cohorts of babies born during the pandemic, such as the mini-COVID study by the European miniNO consortium (https://www.minino-project.com) are thus essential to fully understand the repercussions of these mostly asymptomatic infections on well-aging and to take steps to mitigate them.

A limitation of our study comes from the safety-related, ethical, and organizational challenges posed by the COVID-19 pandemic with regard to the collection of biological samples and the unavailability of human resources for all non-essential clinical research tasks. For example, we measured hormone levels in 3 different cohorts to draw our conclusions: severely ill COVID-19 patients hospitalized in the ICU at the Lille University Hospital, France, an uninfected control group hospitalized in the ICU at Lille but belonging to a different cohort, and finally COVID-19 patients with different degrees of severity of the disease, but not uninfected controls, who were subjected to medium-to-long-term follow up at the Endocrinology Department of the Imperial College Healthcare NHS Trust, London, UK. In addition, by definition, our post mortem brain and olfactory epithelium tissues were obtained from COVID-19 patients who had died of the disease, indicating a degree of infection severity and possibly of neuroinvasion that might be rarer in the surviving population. Finally, the time-course of these changes is unknown (we observed abnormal HPG axis function more than a year after infection in two patients who were normal at the first visit, even though most patients who were abnormal at the first visit had become normal by the second), which will make it hard to pin down causality in a variable human population during an ongoing pandemic. Nevertheless, our findings of abnormal and dying GnRH neurons in all the patient brains at our disposal, the dramatic reduction in GnRH expression, and the incipient correlation between HPG axis function, energy metabolism and cognitive or neurological dysfunction underline the necessity for longitudinal studies in COVID-19 survivors, to anticipate a possible delayed-onset wave of developmental, reproductive, metabolic and mental disorders.

Contributors

S.R. and V.P. designed the study, analysed data, prepared the figures, and wrote the manuscript. F.S., S.N., D.F., CFFC. processed human tissues and performed immunofluorescence and in situ hybridization and qRT-PCR analyses, and all were involved in all aspects of study design, interpretation of results, and manuscript preparation; S.A.C., E.M. and W.D. followed and collected the data from the London cohort. G.T., L.C., C.I.-G. and A.S. prepared tissues and performed immunofluorescence; K.C. performed FACS experiments. A.P, J.E-O, M.M-G, produced the pseudotyped virus; F.T. and C.B. infected FNC-B4 cells with SARS-Cov-2; E.H., M.J., D.D., A.M., G.G. contributed material, J.P., T.L. V.F., R.P., F.P. S.C.J., L.S., J. Dewisme and C.A.-M monitored the Lille cohort and collected clinical samples and data, P.P. performed hormonal assays; S.R., V.P., P.G. and W.D. verified the underlying data. H.M.-F., V.F., M.B., M.M.-C., J.P., K.C., M.S., R.N., C.A.-M, P.P., V.M., P.G. and W.D. were involved in study design, interpretation of results, and preparation of the manuscript. All authors critically read and commented on the manuscript and approved the final version for submission.

Data sharing statement

Code used to generate plots plus related files could be accessed here: https://github.com/sreekala03/Gonado_Covid. All data collected for the study, including raw data other than the one displayed in Tables S1, S2, S4, and S5 of the manuscript and data analysis will be made available to others upon request. All data will be available upon publication of the manuscript, by contacting the corresponding authors.

Declaration of interests

The authors declare no competing interest.

Acknowledgements

The authors are grateful to the LICORNE study group for access to patient brains. The Lille COVID Research Network acknowledges the contribution of residents, medical students, nursing teams, laboratory technicians and clinical research associates throughout the SARS-CoV-2 pandemic. The authors thank the Biological Resources Centre of the Centre Hospitalier de Lille (BB 0033-00030) for providing biological samples from the LICORNE and READIAB cohorts.

This work was supported by European Research Council ERC-Synergy-Grant-2019-WATCH No 810331 (to R.N, V. P, and M.S.), ERC-2016-CoG-REPRODAMH No 725149 (to P.G.), ERC-2018-StG 804236-NEXTGEN-IO (to A.P), the European Union Horizon 2020 research and innovation program No 847941 miniNO (to K.C., V.P. and L.S.), the Fondation pour la Recherche Médicale (FRM) and the Agence Nationale de la Recherche en Santé (No ECTZ200878 Long Covid 2021 ANRS0167 SIGNAL to VP, RJ, FT, MS and RN), the Agence Nationale de la Recherche DistAlz (No. ANR-11-LABEX-0009 to V.P. & F.P.), EGID (No. ANR-10-LABEX-0046 to V.P.), I-SITE ULNE (No. ANR-16-IDEX-0004) and benefited from the technical support of UMS2014-US41. The authors also acknowledge support of the Inserm Cross-Cutting Scientific Program (HuDeCA to P.G.), the ANR-3D Human (ANR-19-CE16-0021-02 to P.G.) and the CHU Lille Bonus H. E.G.M. was funded by an MRC Clinical Training Fellowship and NIHR Clinical Lecturer Award. W.S.D. was funded by an NIHR Senior Investigator Award.

Appendix A. Supplementary data

Supplementary data related to this article can be found at https://doi.org/10.1016/j.ebiom.2023.104784.

References

1 Dierssen M. Down syndrome: the brain in trisomic mode. *Nat Rev Neurosci*. 2012;13(12):844–858.
2 Manfredi-Lozano M, Leysen V, Adamo M, et al. GnRH replacement rescues cognition in down syndrome. *Science*. 2022;377(6610):eabq4515.
3 Casoni F, Malone SA, Belle M, et al. Development of the neurons controlling fertility in humans: new insights from 3D imaging and transparent fetal brains. *Development*. 2016;143(21):3969–3981.
4 Buckley RF, O'Donnell A, McGrath ER, et al. Menopause status moderates sex differences in tau burden: a framingham pet study. *Ann Neurol*. 2022;92(1):11–22.
5 Xiong J, Kang SS, Wang Z, et al. FSH blockade improves cognition in mice with Alzheimer's disease. *Nature*. 2022;603(7901):470–476.
6 Wang M, Roussos P, McKenzie A, et al. Integrative network analysis of nineteen brain regions identifies molecular signatures and networks underlying selective regional vulnerability to Alzheimer's disease. *Genome Med*. 2016;8(1):104.
7 Atwood CS, Bowen RL. The endocrine dyscrasia that accompanies menopause and andropause induces aberrant cell cycle signaling that triggers re-entry of post-mitotic neurons into the cell cycle, neurodysfunction, neurodegeneration and cognitive disease. *Horm Behav*. 2015;76:63–80.
8 Ishii M, Iadecola C. Metabolic and non-cognitive manifestations of Alzheimer's disease: the hypothalamus as both culprit and target of pathology. *Cell Metab*. 2015;22(5):761–776.
9 Prevot V, Tena-Sempere M, Pitteloud N. New horizons: gonadotropin-releasing hormone and cognition. *J Clin Endocrinol Metab*. 2023. dgad319.
10 Hampshire A, Chatfield DA, AM MP, et al. Multivariate profile and acute-phase correlates of cognitive deficits in a COVID-19 hospitalised cohort. *eClinicalMedicine*. 2022;47:101417.
11 Xu E, Xie Y, Al-Aly Z. Long-term neurologic outcomes of COVID-19. *Nat Med*. 2022;28(11):2406–2415.
12 Mavrikaki M, Lee JD, Solomon IH, Slack FJ. Severe COVID-19 is associated with molecular signatures of aging in the human brain. *Nat Aging*. 2022;2:1130–1137.
13 Dewisme J, Lebouvier T, Vannod-Michel Q, Prevot V, Maurage CA. COVID-19 could worsen cerebral amyloid angiopathy. *J Neuropathol Exp Neurol*. 2023;82(9):814–817.
14 Cao X, Li W, Wang T, et al. Accelerated biological aging in COVID-19 patients. *Nat Commun*. 2022;13(1):2135.
15 Al-Aly Z, Xie Y, Bowe B. High-dimensional characterization of post-acute sequelae of COVID-19. *Nature*. 2021;594(7862):259–264.
16 Davis HE, McCorkell L, Vogel JM, Topol EJ. Long COVID: major findings, mechanisms and recommendations. *Nat Rev Microbiol*. 2023;21(3):133–146.
17 Monje M, Iwasaki A. The neurobiology of long COVID. *Neuron*. 2022;110(21):3484–3496.
18 The Lancet N. Long COVID: understanding the neurological effects. *Lancet Neurol*. 2021;20(4):247.
19 Salonia A, Pontillo M, Capogrosso P, et al. Severely low testosterone in males with COVID-19: a case-control study. *Andrology*. 2021;9(4):1043–1052.
20 Salonia A, Pontillo M, Capogrosso P, et al. Testosterone in males with COVID-19: a 7-month cohort study. *Andrology*. 2021;10(1):34–41.
21 Clarke SA, Phylactou M, Patel B, et al. Normal adrenal and thyroid function in patients who survive COVID-19 infection. *J Clin Endocrinol Metab*. 2021;106(8):2208–2220.
22 Vannelli GB, Ensoli F, Zonefrati R, et al. Neuroblast long-term cell cultures from human fetal olfactory epithelium respond to odors. *J Neurosci*. 1995;15(6):4382–4394.
23 Crawford KHD, Eguia R, Dingens AS, et al. Protocol and reagents for pseudotyping lentiviral particles with SARS-CoV-2 spike protein for neutralization assays. *Viruses*. 2020;12(5):513.
24 Sekulic M, Harper H, Nezami BG, et al. Molecular detection of SARS-CoV-2 infection in FFPE samples and histopathologic findings in fatal SARS-CoV-2 cases. *Am J Clin Pathol*. 2020;154(2):190–200.
25 Rhoads DD, Cherian SS, Roman K, Stempak LM, Schmotzer CL, Sadri N. Comparison of abbott ID now, DiaSorin simplexa, and CDC FDA emergency use authorization methods for the detection of SARS-CoV-2 from nasopharyngeal and nasal swabs from individuals diagnosed with COVID-19. *J Clin Microbiol*. 2020;58(8):e00760–e007820.
26 Baratchian M, McManus JM, Berk MP, et al. Androgen regulation of pulmonary AR, TMPRSS2 and ACE2 with implications for sex-discordant COVID-19 outcomes. *Sci Rep*. 2021;11(1):11130.
27 Wu CT, Lidsky PV, Xiao Y, et al. SARS-CoV-2 replication in airway epithelia requires motile cilia and microvillar reprogramming. *Cell*. 2023;186(1):112–130.e20.
28 Muller JA, Gross R, Conzelmann C, et al. SARS-CoV-2 infects and replicates in cells of the human endocrine and exocrine pancreas. *Nat Metab*. 2021;3(2):149–165.
29 Kamle S, Ma B, He CH, et al. Chitinase 3-like-1 is a therapeutic target that mediates the effects of aging in COVID-19. *JCI Insight*. 2021;6(21):e148749.
30 Parkash J, Messina A, Langlet F, et al. Semaphorin7A regulates neuroglial plasticity in the adult hypothalamic median eminence. *Nat Commun*. 2015;6:6385.
31 Belle M, Godefroy D, Couly G, et al. Tridimensional visualization and analysis of early human development. *Cell*. 2017;169(1):161–173.e12.
32 Iwata R, Kiyonari H, Imai T. Mechanosensory-based phase coding of odor identity in the olfactory bulb. *Neuron*. 2017;96(5):1139–11352.e7.
33 Hrabovszky E, Molnar CS, Sipos MT, et al. Sexual dimorphism of kisspeptin and neurokinin B immunoreactive neurons in the infundibular nucleus of aged men and women. *Front Endocrinol (Lausanne)*. 2011;2:80.
34 Hanchate NK, Giacobini P, Lhuillier P, et al. SEMA3A, a gene involved in axonal pathfinding, is mutated in patients with Kallmann syndrome. *PLoS Genet*. 2012;8(8):e1002896.
35 Vanacker C, Trova S, Shruti S, et al. Neuropilin-1 expression in GnRH neurons regulates prepubertal weight gain and sexual attraction. *EMBO J*. 2020;39(19):e104633.
36 Lim JS, Ibaseta A, Fischer MM, et al. Intratumoural heterogeneity generated by Notch signalling promotes small-cell lung cancer. *Nature*. 2017;545(7654):360–364.
37 Clasadonte J, Prevot V. The special relationship: glia-neuron interactions in the neuroendocrine hypothalamus. *Nat Rev Endocrinol*. 2018;14(1):25–44.
38 Herbison AE. A simple model of estrous cycle negative and positive feedback regulation of GnRH secretion. *Front Neuroendocrinol*. 2020;57:100837.
39 Lanser L, Burkert FR, Thommes L, et al. Testosterone deficiency is a risk factor for severe COVID-19. *Front Endocrinol (Lausanne)*. 2021;12:694083.
40 Dhindsa S, Zhang N, McPhaul MJ, et al. Association of circulating sex hormones with inflammation and disease severity in patients with COVID-19. *JAMA Netw Open*. 2021;4(5):e2111398.
41 Cinislioglu AE, Cinislioglu N, Demirdogen SO, et al. The relationship of serum testosterone levels with the clinical course and prognosis of COVID-19 disease in male patients: a prospective study. *Andrology*. 2021;10(1):24–33.
42 Spratt DI, Cox P, Orav J, Moloney J, Bigos T. Reproductive axis suppression in acute illness is related to disease severity. *J Clin Endocrinol Metab*. 1993;76(6):1548–1554.
43 Turner HE, Wass JA. Gonadal function in men with chronic illness. *Clin Endocrinol (Oxf)*. 1997;47(4):379–403.

44 Boehm U, Bouloux PM, Dattani MT, et al. Expert consensus document: European consensus statement on congenital hypogonadotropic hypogonadism–pathogenesis, diagnosis and treatment. *Nat Rev Endocrinol*. 2015;11(9):547–564.
45 Messina A, Langlet F, Chachlaki K, et al. A microRNA switch regulates the rise in hypothalamic GnRH production before puberty. *Nat Neurosci*. 2016;19(6):835–844.
46 Baroncini M, Allet C, Leroy D, Beauvillain JC, Francke JP, Prevot V. Morphological evidence for direct interaction between gonadotrophin-releasing hormone neurones and astroglial cells in the human hypothalamus. *J Neuroendocrinol*. 2007;19(9):691–702.
47 Wray S, Grant P, Gainer H. Evidence that cells expressing luteinizing hormone-releasing hormone mRNA in the mouse are derived from progenitor cells in the olfactory placode. *Proc Natl Acad Sci U S A*. 1989;86(20):8132–8136.
48 Schwanzel-Fukuda M, Pfaff DW. Origin of luteinizing hormone-releasing hormone neurons. *Nature*. 1989;338(6211):161–164.
49 Chachlaki K, Messina A, Delli V, et al. NOS1 mutations cause hypogonadotropic hypogonadism with sensory and cognitive deficits that can be reversed in infantile mice. *Sci Transl Med*. 2022;14(665):eabh2369.
50 Cecon E, Fernandois D, Renault N, et al. Melatonin drugs inhibit SARS-CoV-2 entry into the brain and virus-induced damage of cerebral small vessels. *Cell Mol Life Sci*. 2022;79(7):361.
51 Hoffmann M, Kleine-Weber H, Schroeder S, et al. SARS-CoV-2 cell entry depends on ACE2 and TMPRSS2 and is blocked by a clinically proven protease inhibitor. *Cell*. 2020;181(2):271–280.e8.
52 Prevot V, Dehouck B, Sharif A, Ciofi P, Giacobini P, Clasadonte J. The versatile tanycyte: a hypothalamic integrator of reproduction and energy metabolism. *Endocr Rev*. 2018;39(3):333–368.
53 Quinton R, Hasan W, Grant W, et al. Gonadotropin-releasing hormone immunoreactivity in the nasal epithelia of adults with Kallmann's syndrome and isolated hypogonadotropic hypogonadism and in the early midtrimester human fetus. *J Clin Endocrinol Metab*. 1997;82(1):309–314.
54 de Melo GD, Lazarini F, Levallois S, et al. COVID-19-related anosmia is associated with viral persistence and inflammation in human olfactory epithelium and brain infection in hamsters. *Sci Transl Med*. 2021;13(596):eabf8396.
55 Meinhardt J, Radke J, Dittmayer C, et al. Olfactory transmucosal SARS-CoV-2 invasion as a port of central nervous system entry in individuals with COVID-19. *Nat Neurosci*. 2021;24(2):168–175.
56 Khan M, Yoo SJ, Clijsters M, et al. Visualizing in deceased COVID-19 patients how SARS-CoV-2 attacks the respiratory and olfactory mucosae but spares the olfactory bulb. *Cell*. 2021;184(24):5932–5949.e15.
57 Khan M, Clijsters M, Choi S, et al. Anatomical barriers against SARS-CoV-2 neuroinvasion at vulnerable interfaces visualized in deceased COVID-19 patients. *Neuron*. 2022;110(23):3919–39135.e6.
58 Giacobini P, Parkash J, Campagne C, et al. Brain endothelial cells control fertility through ovarian-steroid-dependent release of semaphorin 3A. *PLoS Biol*. 2014;12(3):e1001808.
59 Marcos S, Monnier C, Rovira X, et al. Defective signaling through plexin-A1 compromises the development of the peripheral olfactory system and neuroendocrine reproductive axis in mice. *Hum Mol Genet*. 2017;26(11):2006–2017.
60 Cantuti-Castelvetri L, Ojha R, Pedro LD, et al. Neuropilin-1 facilitates SARS-CoV-2 cell entry and infectivity. *Science*. 2020;370(6518):856–860.
61 Daly JL, Simonetti B, Klein K, et al. Neuropilin-1 is a host factor for SARS-CoV-2 infection. *Science*. 2020;370(6518):861–865.
62 Crunfli F, Carregari VC, Veras FP, et al. Morphological, cellular, and molecular basis of brain infection in COVID-19 patients. *Proc Natl Acad Sci U S A*. 2022;119(35):e2200960119.
63 Wenzel J, Lampe J, Muller-Fielitz H, et al. The SARS-CoV-2 main protease M(pro) causes microvascular brain pathology by cleaving NEMO in brain endothelial cells. *Nat Neurosci*. 2021;24(11):1522–1533.
64 Franssen D, Barroso A, Ruiz-Pino F, et al. AMP-activated protein kinase (AMPK) signaling in GnRH neurons links energy status and reproduction. *Metabolism*. 2021;115:154460.
65 Fodoulian L, Tuberosa J, Rossier D, et al. SARS-CoV-2 receptors and entry genes are expressed in the human olfactory neuroepithelium and brain. *iScience*. 2020;23(12):101839.
66 Maggi M, Barni T, Fantoni G, et al. Expression and biological effects of endothelin-1 in human gonadotropin-releasing hormone-secreting neurons. *J Clin Endocrinol Metab*. 2000;85(4):1658–1665.
67 Fenizia C, Biasin M, Cetin I, et al. Analysis of SARS-CoV-2 vertical transmission during pregnancy. *Nat Commun*. 2020;11(1):5128.
68 Facchetti F, Bugatti M, Drera E, et al. SARS-CoV2 vertical transmission with adverse effects on the newborn revealed through integrated immunohistochemical, electron microscopy and molecular analyses of Placenta. *eBioMedicine*. 2020;59:102951.
69 Matschke J, Lutgehetmann M, Hagel C, et al. Neuropathology of patients with COVID-19 in Germany: a post-mortem case series. *Lancet Neurol*. 2020;19(11):919–929.
70 Song E, Zhang C, Israelow B, et al. Neuroinvasion of SARS-CoV-2 in human and mouse brain. *J Exp Med*. 2021;218(3):e20202135.
71 Yang AC, Kern F, Losada PM, et al. Dysregulation of brain and choroid plexus cell types in severe COVID-19. *Nature*. 2021;595(7868):565–571.
72 Stein SR, Ramelli SC, Grazioli A, et al. SARS-CoV-2 infection and persistence in the human body and brain at autopsy. *Nature*. 2022;612(7941):758–763.
73 Douaud G, Lee S, Alfaro-Almagro F, et al. SARS-CoV-2 is associated with changes in brain structure in UK Biobank. *Nature*. 2022;604(7907):697–707.
74 Fernandez-Castaneda A, Lu P, Geraghty AC, et al. Mild respiratory COVID can cause multi-lineage neural cell and myelin dysregulation. *Cell*. 2022;185(14):2452–2468.e16.
75 Butowt R, von Bartheld CS. The route of SARS-CoV-2 to brain infection: have we been barking up the wrong tree? *Mol Neurodegener*. 2022;17(1):20.
76 Facondo P, Maltese V, Delbarba A, et al. Case report: hypothalamic amenorrhea following COVID-19 infection and review of literatures. *Front Endocrinol (Lausanne)*. 2022;13:840749.
77 Soejima Y, Otsuka Y, Tokumasu K, et al. Late-onset hypogonadism in a male patient with long COVID diagnosed by exclusion of ME/CFS. *Medicina (Kaunas)*. 2022;58(4):536.
78 Lebar V, Lagana AS, Chiantera V, Kunic T, Lukanovic D. The effect of COVID-19 on the menstrual cycle: a systematic review. *J Clin Med*. 2022;11(13):3800.
79 Lechien JR, Chiesa-Estomba CM, De Siati DR, et al. Olfactory and gustatory dysfunctions as a clinical presentation of mild-to-moderate forms of the coronavirus disease (COVID-19): a multicenter European study. *Eur Arch Otorhinolaryngol*. 2020;277(8):2251–2261.
80 Hellier V, Brock O, Candlish M, et al. Female sexual behavior in mice is controlled by kisspeptin neurons. *Nat Commun*. 2018;9(1):400.
81 Zhang G, Li J, Purkayastha S, et al. Hypothalamic programming of systemic ageing involving IKK-beta, NF-kappaB and GnRH. *Nature*. 2013;497(7448):211–216.
82 Herbison AE, Porteous R, Pape JR, Mora JM, Hurst PR. Gonadotropin-releasing hormone neuron requirements for puberty, ovulation, and fertility. *Endocrinology*. 2008;149(2):597–604.
83 Nampoothiri S, Nogueiras R, Schwaninger M, Prevot V. Glial cells as integrators of peripheral and central signals in the regulation of energy homeostasis. *Nat Metab*. 2022;4(7):813–825.
84 Kwan AC, Ebinger JE, Botting P, Navarrette J, Claggett B, Cheng S. Association of COVID-19 vaccination with risk for incident diabetes after COVID-19 infection. *JAMA Netw Open*. 2023;6(2):e2255965.
85 Schultheiss C, Willscher E, Paschold L, et al. The IL-1beta, IL-6, and TNF cytokine triad is associated with post-acute sequelae of COVID-19. *Cell Rep Med*. 2022;3(6):100663.
86 Mehandru S, Merad M. Pathological sequelae of long-haul COVID. *Nat Immunol*. 2022;23(2):194–202.
87 Bottcher M, Muller-Fielitz H, Sundaram SM, et al. NF-kappaB signaling in tanycytes mediates inflammation-induced anorexia. *Mol Metab*. 2020;39:101022.
88 Figueiredo CPF-DF, da Poian AT, Clarke JR. SARS-CoV-2-associated cytokine storm during pregnancy as a possible risk factor for neuropsychiatric disorder development in post-pandemic infants. *Neuropharmacology*. 2021;201:108841. https://doi.org/10.1016/j.neuropharm.2021.
89 Villar J, Ariff S, Gunier RB, et al. Maternal and neonatal morbidity and mortality among pregnant women with and without COVID-19 infection: the INTERCOVID multinational cohort study. *JAMA Pediatr*. 2021;175(8):817–826.

90 Pellegrino G, Martin M, Allet C, et al. GnRH neurons recruit astrocytes in infancy to facilitate network integration and sexual maturation. *Nat Neurosci*. 2021;24(12):1660–1672.

91 Kuiri-Hanninen T, Kallio S, Seuri R, et al. Postnatal developmental changes in the pituitary-ovarian axis in preterm and term infant girls. *J Clin Endocrinol Metab*. 2011;96(11):3432–3439.

92 Kuiri-Hanninen T, Seuri R, Tyrvainen E, et al. Increased activity of the hypothalamic-pituitary-testicular axis in infancy results in increased androgen action in premature boys. *J Clin Endocrinol Metab*. 2011;96(1):98–105.

93 D'Onofrio BM, Class QA, Rickert ME, Larsson H, Langstrom N, Lichtenstein P. Preterm birth and mortality and morbidity: a population-based quasi-experimental study. *JAMA Psychiatry*. 2013;70(11):1231–1240.

94 Luu TM, Katz SL, Leeson P, Thebaud B, Nuyt AM. Preterm birth: risk factor for early-onset chronic diseases. *CMAJ*. 2016;188(10):736–746.

95 Mulkey SB, Williams ME, Jadeed N, Zhang A, Israel S, DeBiasi RL. Neurodevelopment in infants with antenatal or early neonatal exposure to SARS-CoV-2. *Early Hum Dev*. 2022;175:105694.